Load Side Detection of Series Arcs in DC Microgrids by Simulation and Experimental Validation

Zhihao Liu

Master of Science Thesis

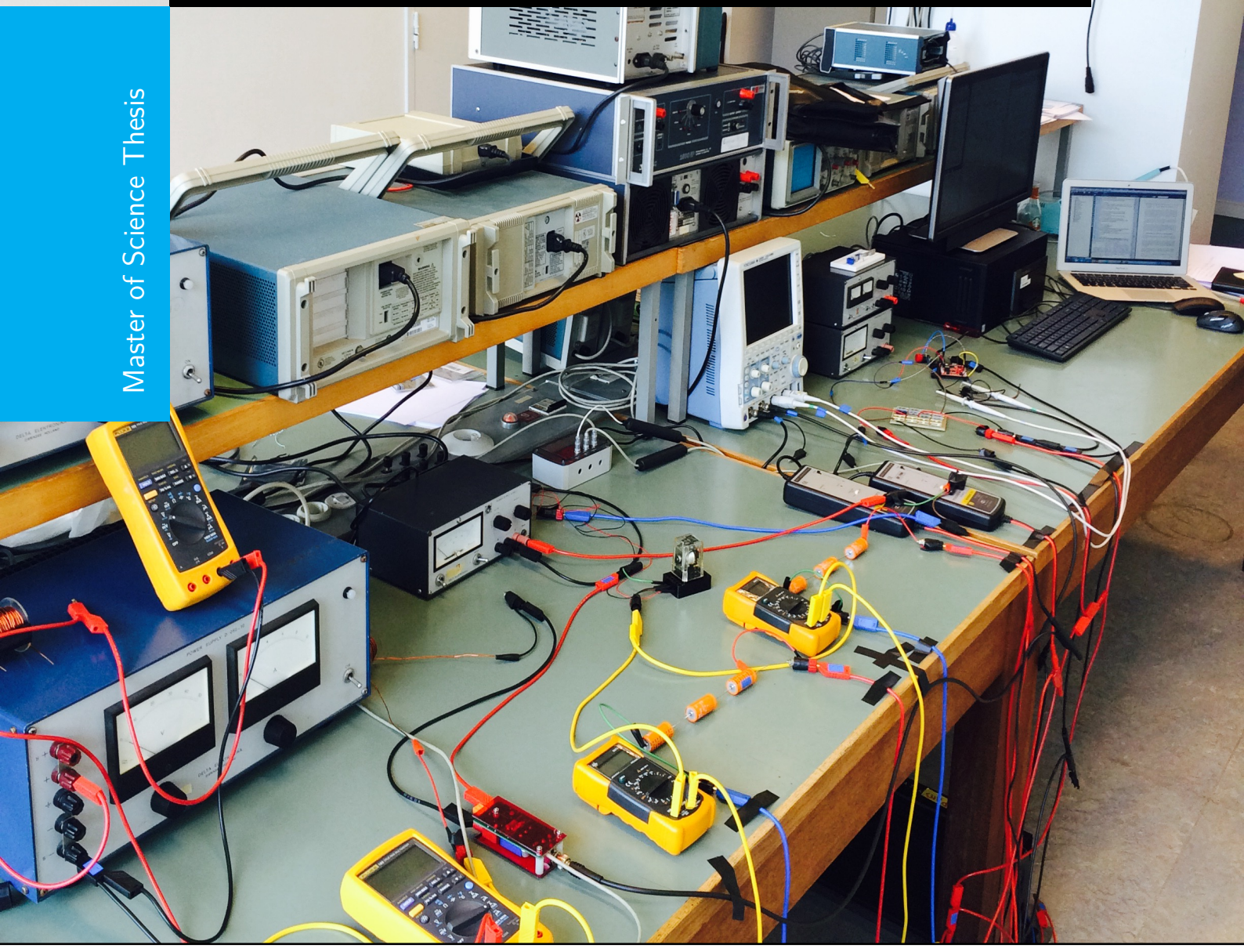

TU Delft Delft University of Technology

Electrical Sustainable Energy

Load Side Detection of Series Arcs in DC Microgrids by Simulation and Experimental Validation

Master of Science Thesis

For the degree of Master of Science in Electrical Power Engineering at Delft University of Technology

Zhihao Liu

Supervisors:

Prof. dr.ir. L.M. Ramirez Elizondo
Prof.dr.eng. P. Bauer

August 22, 2016

Faculty of Electrical Engineering, Mathematics and Computer Science (EEMCS)

TU Delft Delft University of Technology

DCE&S DC systems, Energy conversion & Storage

Delft University of Technology
Department of
Electrical Sustainable Energy (ese)

The undersigned hereby certify that they have read and recommend to the Faculty of Electrical Engineering, Mathematics and Computer Science (EEMCS) for acceptance a thesis entitled

Load Side Detection of Series Arcs in DC Microgrids by Simulation and Experimental Validation

by

Zhihao Liu

in partial fulfillment of the requirements for the degree of

Master of Science Electrical Power Engineering

Dated: August 22, 2016

Supervisor(s):

Prof. dr.ir. L.M. Ramirez Elizondo

Prof.dr.eng. P. Bauer

Mr. Aditya Shekhar

Reader(s):

Prof. dr.ir. Jose L. Rueda Torres

Abstract

With increasing scale of usage for renewable energy resource, DC micro-grids system becomes more and more popular for the application of different kinds of power electronics in DC. However DC arc fault introduces major safety concerns due to the randomness and instability, especially absence of zero current crossing, which makes it is hard to be detected and eliminated. In this thesis, a novel proposed series dc arc detection methods were validated both in theoretical simulation by MATLAB and in real-time experiments by creating real arcing in the constructed equivalent DC system. By changing the parameters and type of both the circuit and the setting of detection method, the arc detection performs with sensitivity, selectivity, speed and reliability harvested. Additionally, the research and practical tests have also been conducted to study the characteristics of series dc arc, which contributes to the determination of the appropriate setting value for the arc detection algorithm.

Table of Contents

List of Figures

List of Tables

Acknowledgements

This thesis represents not only my work at the keyboard, and it is a milestone in my life.

First and foremost, I would offer my sincerest gratitude to my supervisor, Prof.Bauer and Prof.Elizondo, who have supported me throughout my thesis with their patience, enthusiasm, motivation and immense knowledge. I attribute the level of my Masters Degree to their encouragement and effort.

Besides my supervisor, I would like to thank the rest of my thesis committee: Dr.ing.Torres for his encouragement, insightful comments.

My sincere thanks also goes to M.Sc. Aditya for leading me in the research and supporting me to accomplish all the tremendous simulation and experiments works. Without him, I could not reach this level in academic and skills.

In addition, I would like to thank the technicians in $DCE\&S$ lab, Bart, Joris, Harrie and Chris. You definitely provided me with the equipments that I required for the experiments and advice about the better methods to achieve successes in my experiments.

I would also like to thank my friends: Yuxuan Li, Ting Zhang, Yue Ma, Jianzhao Wei, Ruo Jia, Zhiqin Lin. They give me the encouragement when I felt frustrated and provide their best assist when I was in urgent. They let me know that the true friend will accept everything of you, no matter the merits or demerits. All of you are my treasured friend forever.

Last but not the least, I must express my very profound gratitude to my parents: Shumin Wang and Nailu Liu, for giving birth to me and raising me up and for providing me with unfailing support both in financial and spiritual and continuous encouragement throughout my years of study and through the process of researching and writing this thesis. This ac-

complishment would not have been possible without them. I love you!

Delft, University of Technology Zhihao Liu
August 22, 2016

自信人生二百年，会当水击三千里

I believe I can fly

Chapter 1

Thesis Outline and Research Objectives

Among the different kinds of reasons why there is an increasing trend of application of Direct Current (dc) micro-grids system in power electronics system, the most important one is that the ease of integration with renewable energy resource and the energy storage units, which meets the demand of the direction for the development of future power systems [1].

While dc micro-grids offer many advantages, challenges still remain.

The randomness and instability of series dc arc makes it is difficult to be detected and series dc arc is quite hard to be extinguished automatically as there is no zero crossing of current during the normal operating condition. This can cause damage to the system and the endanger the equipment attached. protection issues have hindered the widespread of the dc micro-grids [2].

DC arc fault introduces major safety concern in a wide variety of power electronic applications. As a consequence, a reliable, accurate and speedy series dc arc detection method is needed to solve these issues and to open the door of future for the dc micro-grids systems.

The work described in this thesis aims to investigate the arc characteristics and develop an arc detection method, which will then be applied to detect the series arc faults by measuring some general electrical quantities, as a consequence the power electronic converter can be controlled to take suitable actions to prevent or significantly reduce the damage caused by arc fault and improve the safety of the DC micro-grid system.

As for the project about the series arcing detection method development and validation,

the following research questions are addressed:

- How rapid and selective is the designed series arc detection algorithm to arcing at point of common coupling?
- What is the influence of circuit parameters (V, I, L, C) on the series arc behavior and measured load voltage practically?
- How does the designed arc detection algorithm respond to series arcs in terms of sensitivity and selectivity experimentally?
- What is the impact of varying system conditions and set threshold voltage on the sensitivity and selectivity of the arc detection algorithm?

In this thesis, the proposed arc detection algorithm is described and validated both through simulations and experiments to show the selectivity and sensitivity when the arc fault is initiated at DC-side of the circuit network.

The experiments is designed to determine the influence on the characteristics of the series dc arc by changing value of the dc source voltage, the load current, the cable inductance and the input load capacitance. Based on the experimental data, the results would be depicted to show the different response of the series dc arc under different conditions of circuit parameters, which would offer more information for setting the triggering value of the series dc arc detection method.

Chapter 2

Motivation

Nowadays, apart from air and water, energy has become a basic necessity of daily life.

Along with the rapid development of the modern society, more and more energy is needed to meet the growing demands of the human beings. However, the main source of energy used today is fossil fuel which not only reduces day by day, but also causes seriously environmental pollution that has already threaten the safety of life on Earth.

With the properties of greenness and sustainability, the renewable energy resources such as wind, solar and tide are now receiving more and more attention. To cope with the issues caused by the conventional fossil energy, many governments in the world have published out the energy policy in order to increase the requirement of the penetration of renewable energy resources among the total energy consumed. For instance, the California government U.S., would increase the usage of renewable generation up to around 33% by 2020 [3].

Since the increasing demand of energy would bring in some new problems like heavy power cuts and also many people live in the remote or rural area which are disconnected from the central power supply grid, an isolated electric power system micro-grid technologies appears to solve these problems proposed before [1].

LV distribution systems with distributed energy resources (micro-turbines, PV, fuel cells, etc.) together with energy storage devices (batteries, energy supercapacitors and flywheels) and flexible loads, micro-grids can be operated either in a non-autonomous way, if interconnected to the grid, or in an autonomous way, if disconnected from the main grid [4]. The operation and management of micro-sources in the network can provide distinct benefits to the performance of the overall system, if managed and coordinated effectively and efficiently.

Micro-grid is an integration platform for supply-side (microgeneration), storage units and demand resources (controllable loads) located in a local distribution grid, and a micro-grid should be capable of handling both normal state (grid-connected) and emergency state (islanded) operation. While micro-grid penetrated by micro-sources lies mainly in terms of management and coordination of available resources, which make is different from a passive grid [5].

Being regarded as a bridge between the traditional centralized grid and the future distributed and real-time power demand grid, micro grids are becoming more and more popular.

Because these is no impacts of proximity effect and skin effect which usually happen in the Alternating Current (ac) condition [5], the dc micro-grid also shows the high potential for improving the flexibility and ability of the electronic utilities and boosting the compatibility of power load which has made the dc micro-grid to be the optimum solution to have the ease integration with renewable energy sources and the energy storage devices.

Although the power electronics units and conversions are simplified in dc micro-grids, the system protection also attracts more attention due to the absence of zero crossing of the current [6]. In order to ensure the reliable operation of the DC micro-grid, it is important to study the faults may occur during operating period. In the DC micro-grid, the position of fault may change from the bus line to any feeder lines [7], the possible faults can be sorted into three different types:

1. the pole-to-pole short circuits faults usually with low fault impedance;
2. the pole-to-ground short-circuits faults with either low or high impedance;
3. the arc faults.

Based on the location with respect to the load, the arc faults can be divided into two categories: series arc and parallel arc [8]. Between these two types of faults, the series arc fault which is defined by arc being in series with the load is more common [9]. Thus this thesis will focus on the series arc by designing and building the experiment setup to investigate the arc characteristic and proposing the arc detection algorithm which will be verified both in theoretically and experimentally.

The series arc faults occur accidentally at unintended points of discontinuity in the electrical system as the result of the contactors separation may be caused by the imperfections such as loosing connector, aging cable splices and insulation deterioration.

Since there is no current zero-crossing, the series dc arc will be more sustainable.

If the arc fault cannot be detected and eliminated in time, the detrimental impact of arc

would spread to the circuit in vicinity and put the power source and electrical utilities in danger which may lead to hazards such as electrical fires and cause significant damage on electrical system and even loss of both property and human lives.

However the difficulties in arc fault detection, location and elimination has confined the widespread application of dc micro-grids system. As a result of the complex profile and high impedance nature, arc faults cannot be recognized by the conventional current protection equipment [9].

By sensing the current variation, noise, infrared radiation and electromagnetic radiation, many researches of detection method in time domain has been done, which requires that the sensor used in these methods should be in highly sensitivity, however as a consequence is quite vulnerable to the noise interference in the ambience [10, 11, 12].

Some other detection methods for DC arc based on frequency analysis has been developed in the [13, 14, 15]. These detection methods focus on the characteristic of a dc arc but also introduce other problems into arc detection when the issues of noise recognition, calculation time reduction or differentiation from load changes cannot be treated appropriately.

Although many methods for dc arc detection have been studied, a cost-effective solution is still needed to detect and localize the arc fault reliably, accurately and speedily.

This thesis focuses on the study on the new proposed series dc arc detection algorithm [16], and both simulative and practical validation will be developed and performed to prove that the reliability, sensitivity and rapidity can be achieved, which would meet the requirements for series dc arc detecting. In order to make the study more complete, a series of experiments will be conducted to investigate the influence of characteristics of the series dc arc while changing the circuit parameters.

Chapter 3 will make an necessary introduction to the electrical arcs, some basic knowledge about arc, especially the electrical properties were explained in detail. Additionally, some description and analysis have been conducted both on the advantages and disadvantages of some representative dc arc detection methods.

The proposed series dc arc detection algorithm [17] will be explained in Chapter 4, and the theoretical validation will be performed by simulation in MATLAB by building the modeling of equivalent circuit, which is expected to show the selectivity and localization when the series dc arc fault were initiated at the DC-side in the dc micro-grids system especially under the condition of two constant power loads connected in parallel, while guarantee the speed.

In Chapter 5, some research on the series dc arc properties, like arc generation and sustainability will be designed and developed via varying the circuit parameters including the

dc source voltage, the load current, the grid inductance and the input load capacitance to discuss the impact of the external factors on the characteristics of the series dc arc, and the load-side voltage drop and the corresponding time which are associated with the arc initiation.

The validation of the proposed series dc arc detection algorithm will also be conducted in real time experiments via programming the micro-controller with the detection method to present the applicability in the detection for real arc fault in the power system network under different circuit parameters. Moreover, by changing the set value of the trigger voltage of the arc detection algorithm, the influence of the threshold voltage on the detection process will be depicted. In Chapter 6, the whole story is waiting to be told.

The conclusion and future work will be drawn in Chapter 7.

Chapter 3

Introduction

In this Chapter, the basic knowledge about the creation and extinction of electric arc has been explained, especially in the context of electrical characteristics. Moreover, some discussion has been made among different kinds of representative arc detection methods which have already been applied in the normal operation of dc micro-grids system so far.

3-1 Creation and Extinction of Electric Arcs

The electric arc is a plasma channel between the breaker contacts after a discharge in the extinguishing medium and form a self-sustaining discharge of electricity in a conductive ionized gas like shown in Fig.3-1, which often occurs in the electrical system [3].

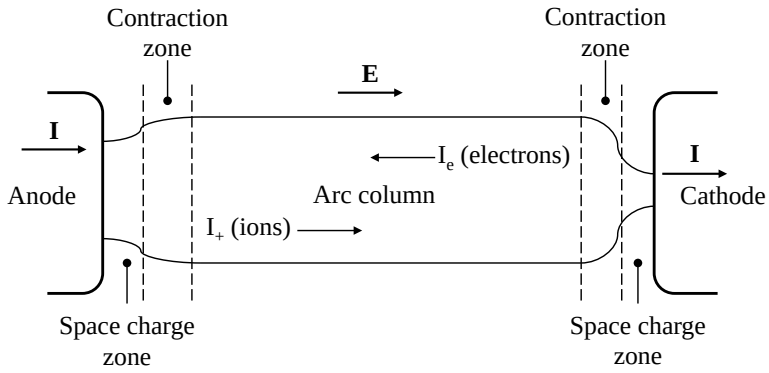

Figure 3-1: The schematic diagram for arcing process.

When a current flows through a circuit breaker and the contacts of the breaker part, the

magnetic energy stored in the inductances of the power system forces the current to continue flowing. Just before contact separation, the breaker contacts touch each other at a very small surface area, resulting in high current density which makes the contact material to vaporize. This leads to a gas discharge in the surrounding medium, which will provide energy to the molecule in surrounding medium and produce heat [18]. With increasing heat, the molecules in surrounding medium become more and more active [4]. Finally, giving rise to highly conductive plasma [2]. Since the free electrons and the heavier positive ions in the high temperature plasma channel, the plasma channel is highly conducting and the current continues to flow after contact separation. Because of the potential difference between the contacts is quite small and the arc will be maintained by the sufficient energy provided by electrical system [18].

The electric arc works as a low resistance path in a circuit breaker, which plays the key role in the interruption process and is therefore often addressed as arc extinction [2].

It is essential to know that the ionised particles between the electrode contactors are the two key factors which is responsible for the creation and maintenance of series dc arc in LV [18].

The arc is much easier to initiate and maintain when the contacts have a small separation. As a result the principles to extinguish the arc are to separate electrode contactors to such a distance that ionized particles become inadequate to maintain the arc, and to deionized the arc path to will be facilitate the arc extinction process which can be achieved by cooling the arc or by bodily removing the ionized particles from the space between the electrode contactors [18].

3-2 Electrical Characteristics of Series DC Arc

Arc is a complex physical phenomenon with its internal characteristic are based on the equations of fluid dynamics and obey the laws of thermodynamics in combination with Maxwell's equations, which makes the arc equations complex [19]. Considering that arcing is a stochastic process with a large number of unknowns, its electrical characteristics will be statistically studied [18].

As for the analysis in level of electrical characteristics, the parameters such as arc resistance, arc voltage and arc current will be used to represent the electrical behaviour of arc to help us better understand the arc behaviour as a part of power system.

Fig.3-2 illustrates a typical series dc arc waveforms, including the key traits of arc voltage and arc current.

- Arc Voltage (V_{arc})

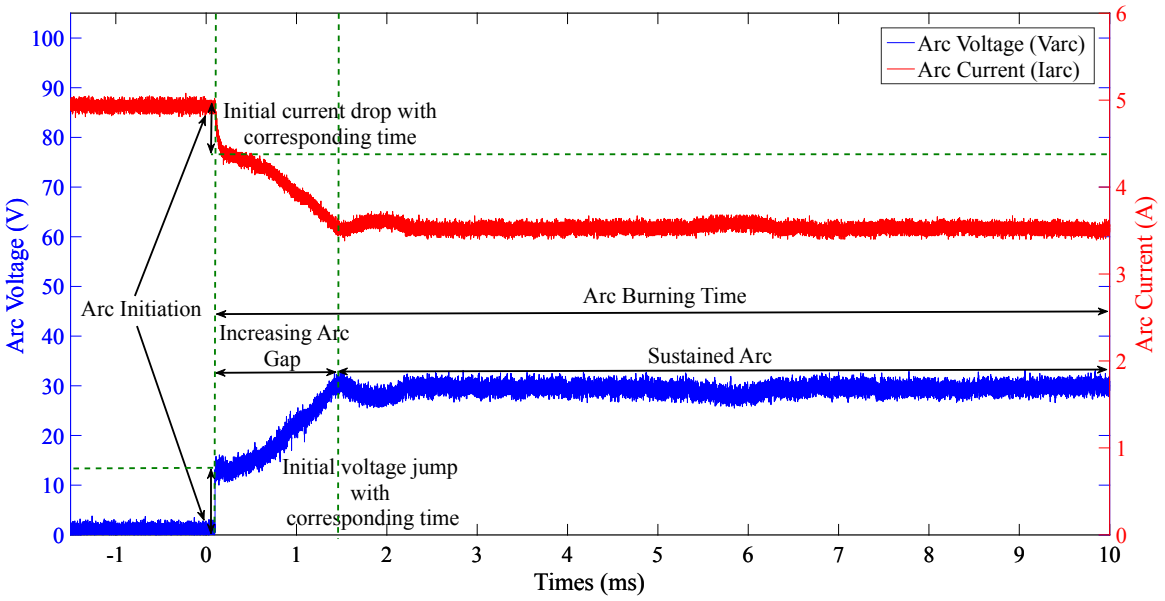

Figure 3-2: The characteristics of voltage and current for series dc arc.

At the beginning of the arc initiation, the arc voltage instantly increases to a minimal value which is the minimal voltage to initiate an electric arc for the specific contactors material [2, 20]. The minimal arc voltage is determined by the electrode material and is independent of the value of supply voltage, arc current and electrode gap length [21].

As the electrode gap continues to grow, arc voltage increases with gradient which is also independent of dc source voltage [3]. When the gap length becomes constant, then the arc voltage becomes constant and a sustained arc is obtained.

- Arc Current (I_{arc})

  When the initiation of arc starts, a slightly reduction immediately happens to the arc current [2]. However the negligible variation caused by the series arc fault appears in the dc circuit is hard to be detected by the current protection unites. In case of constant resistance load, as the arc voltage increases with a constant gradient, the arc current will decreases with a according gradient related to the increasing gradient of arc voltage [3, 20], and enter into constant value at the same moment when the arc voltage becomes constant.

- Arc Resistance (R_{arc})

  In general, arc is supposed to be resistive and the arc resistance is nonlinear due to the most adoption of the macroscopic V-I equation of arc [2]. Thus, all cases of arcing condition should be obtained and more accumulation of experimental results and according models are required to obtain the V-I characteristic of arc shows an inversion relationship and changes significantly under different arcing conditions, which has made a better understanding of the arc behaviour as a part of an electrical system [5].

3-3 Influencing Factor on the Characteristics of Series DC Arc

The main factors which could have influence on the external characteristics of the series dc arc are composed of the temperature, properties of electrode including the electrode material, the electrode gap length, the electrodes separation speed and the electrode geometry and the parameters of power system such as dc source voltage, load current level, grid inductance and the load-side capacitance [18].

Since the arc length is difficult to measure, a number of papers [2, 3, 4, 10, 21, 22] consider the electrode gap length as arc length when the arc current is low and electrode gap is short, as a consequence the assumptions also have been made in this thesis that the arc length is equal to the electrode gap length.

- Arc Voltage (V_{arc})

  The relation between the arc voltage versus dc source voltage shows a stable tendency with the increasing level of external dc source voltage when the load current level is high, while the trend of arc voltage shows higher value with larger gap length under all load current levels [23]. There is also a strong dependence of arc voltage on the arc current [2]. The arc voltage gives different values at different arc gap length and different load current level [3, 23].

- Arc Current (I_{arc})

  Moreover, the current variation tends to decrease with higher dc source voltage which indicates that although the dc source voltage has little impact on the arc voltage and arc resistance, higher dc source voltage has the ability to suppress the chaotic nature of dc arc in certain degree which can stabilize the arc current and make the current variation lower [3].

- Arc Resistance (R_{arc})

  The dc source voltage has a slight effect on the arc resistance [23], while the load current shows a more significant influence to the arc resistance, especially when the level of current is low, the higher load current the lower the arc resistance. Arc resistance tends to rise as the electrode gap length grows [3]. The electrode material also has influence on the resistance of arc [4].

Based on the condition of electrode gap length, the series dc arc faults can be sorted into three types [6]: constant gap length, constant-speed gap, accelerated-speed gap:

1. Constant gap length fault are series faults where the electrodes remain stationary after reaching a predetermined distance. Most arc models in literature assume this fault type;

2. Constant-speed series faults represent conductors tearing longitudinally at a constant speed;

3. Accelerated series faults represents the separation of two conductor section at an accelerated rate.

The electrode gap distance has an obvious impact on the average arc current, which shows that increasing electrode gap length can accelerate the quench of arc. However the electrode diameter has little effect on arc current except in a longer gap distance larger than $0.5cm$ [2]. As for the moving speed of the electrode, arc current variation amplitude increase as the electrode separation speed becomes faster, which will cause a huge current mutation in power system and a detrimental impact on the insulation of the power equipment and transmission line at a very fast separation moving speed [5].

For an arc with a fixed length, in the low current region, the arc current increases as the arc voltage drops, which indicates that the arc power tends to remain steady. Both the dc source voltage level and the load current level have influences to the arc current variation. For higher load current level, the current variation is larger.

In a practical dc micro-grids system, the gird inductance and load side capacitance in the system will have an impact on the creation of the arcing via changing the dynamic process before and during the arc inception [17], meanwhile the current density of the contactors and the electrical field between the separated electrode contactors gap also posed some influences in a certain level on the characteristics of series dc arc, which may result in new development or improvement for the series dc arc detection methods.

3-4 Evolution of the Series DC Arc Detection Methods

In most situations, arc exists in the system as a fault. Arc faults can be divided into two categories: series arc and parallel arc [7]. Series arc fault is defined by the arc being in series with the load.

As a result of degradation of contacts, for example, a connector block due to vibration, poor assembly or damage, series dc arc fault can occur accidentally at arbitrary location of any dc system with high voltage dc bus [10, 11], the arc channel is associated with complex profiles and high impedance and therefore causes lower fault current than nominal current. This adds significant difficulties to traditional arc fault interrupter and majority of dc protection strategies.

It is already know that dc arc faults, in contrast of AC arc, as there are no zero-crossing of current, DC arc is difficult to quench and if not detected and extinguished on time will causes detrimental effect on the power source and control circuits, even leads fire hazards and endanger the whole system.

Therefore, it is vital to detect arc faults in power systems, although the series dc arc faults can

be difficult to detected and locate due to their randomness, intermittent and chaotic nature.

Studies on the series dc arc detection mainly focused in both time and frequency domain [12, 24].

DC arc detection methods based on time domain signatures depend mostly on the signal of arc current. They involve relatively simple calculation procedures but require more measures for avoiding the nuisance tripping. Current drop is used in [13] as a sign of precursor to dc arc, so that it can be prevented right after the air gap is formed and before arc fault is even developed. In [14], a fast change in the slope of voltage or current over time is considered as an arcing event. Moreover, authors in [15] propose a different detection method, where the current will be cut off momentarily and then connected back after sensing a current reduction. The current profile will be different when the current reduction is caused by an arc instead of normal operation.

In [12, 25], statistical methods are adopted to identify arc by studying the variation of the arc voltage and the current signal, voltage and current sensors at two different location in the electrical circuit are utilized to detect anomalies caused by dc arcs.

However these solutions require special device designs and additional components which can be easily influenced by the surrounding electromagnetic environment.

And many dc arc detecting methods based on frequency characteristic of dc arc has been present. In [24], back propagation neural network analysis is used along with a fast frequency transform (FFT) method in order to detect dc arc in spacecraft systems In [11], wavelet packet analysis which has the localization characteristic is applied in arc detecting based on the dc arc energy in different sub-bands is quantified into one variable by using the reconstruction coefficients in each band. Although the problem in sensor is avoided, however, in dc distribution, this simple method cannot be directly applied since a large range of switching power circuits for multi-sources and loads operate all together. The operation of the multiple sources and loads could confuse the arc fault detector and may cause false-positives, which makes arc detection in dc systems full of challenging, such as noise jamming, algorithm optimization, calculation time reduction, differentiation caused by grid source fluctuation or load changes, etc. [13, 25].

Although many efforts has been dedicated into developing the useful detection method of series dc arc, more advanced algorithms on detecting series arc fault deserve further study to achieve both the reliability and the selectivity.

In the next chapter, aiming to improve the detection reliability and suppress false-positives, a new arc fault detection algorithm is explained and discussed.

Chapter 4

Theoretical Simulation and Validation of Arc Detection Algorithm

In this chapter, the proposed arc detection method [16, 17] has been explained, and then the modeling of the proposed series dc arc detection and elimination algorithm have been validated in the equivalent circuit built for the dc micro-grids system with loads by applying the MATLAB Simulink.

4-1 Proposed Arc Detection Method

The reliable arc detection as what was discussed in the Chapter 3 can be achieved by applying the method making use of the electrical characteristics of the arc.

Fig.4-1 illustrates response of load voltage and load current to the transition from no arc to a sustained series dc arc in a dc micro-grids system with constant resistance load. During arc inception, both load voltage and load current vary obviously at the moments of the arc initiating.

The series dc arc detection algorithm adopted in this thesis project is based on the sensing the load-side voltage drop caused by the arc initiation.

As mentioned above, the initial rise of the arc voltage is specially determined by the electrode contact material [21] (more information is given in Table.4-1) and is independent of the supply dc source voltage, and the voltage drop associated with the arc initiation in the load side can be detected by the load-side power electronic devices, which can be used to trigger the action of the current controllable units to ramp the load current to zero in order to disconnect the arcing load and to eliminate the arc quickly without interrupting other parallel loads.

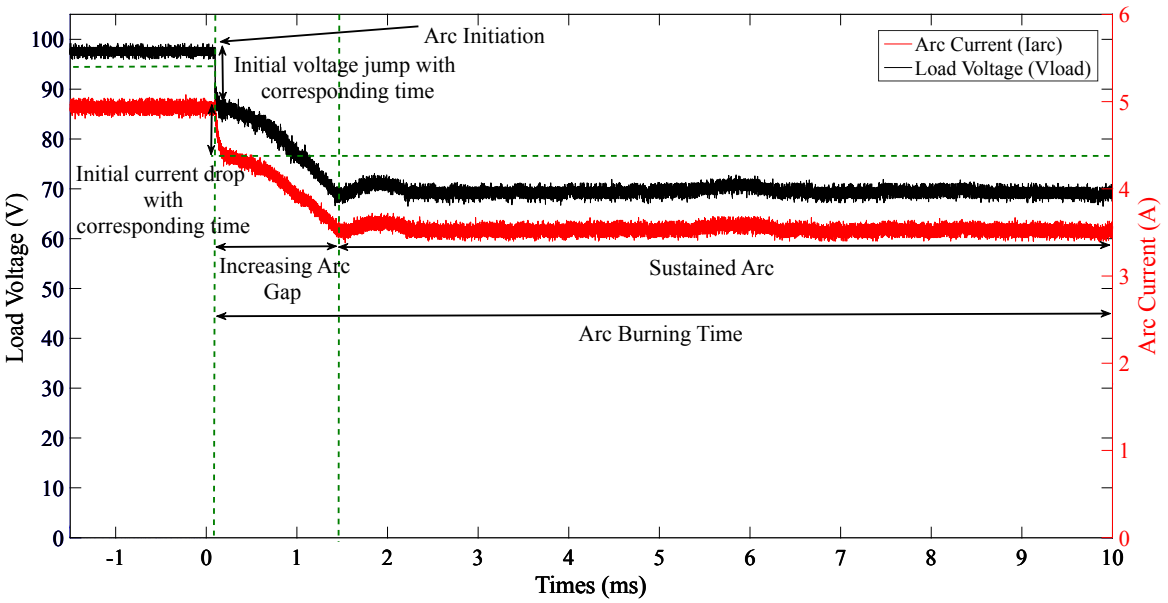

Figure 4-1: The response of load voltage to series dc arc fault.

Table 4-1: Minimal Arc Voltage in Air [21].

Electrode materials	Cu	Au	Ag	Pt
V_{m} (V)	13	15	12	17.5
Average V_{m} (V)	13.3	14.8	11.9	17.7

The proposed series dc arc detection algorithm [16, 17] is depicted in Fig.4-2, in which the load voltage V_{load} is detected and passed through two different Low Pass Filter (LPF) as shown in 4-1 and 4-2, with Laplace transfer functions:

$$V_{\mathrm{slp}}(s) = \left(\frac{1}{1+\tau_{\mathrm{s}}s}\right) V_{\mathrm{load}}(s) \tag{4-1}$$

$$V_{\mathrm{flp}}(s) = \left(\frac{1}{1+\tau_{\mathrm{f}}s}\right) V_{\mathrm{load}}(s) \tag{4-2}$$

It is noteworthy that the choice of the time constant for Slow LPF (τ_{s}) and Fast LPF (τ_{f}) should take some issues into consideration, such as the speed to reach the steady state, the noise interference from both the grid voltage fluctuation and the switching ripple. The Slow LPF and Fast LPF can compose a band pass filter only to let the special frequency in the bandwidth can be detected [26]. Then, as shown in 4-3 when the value of ΔV in 4-3, the difference between the outputs voltages V_{slp} and V_{flp} from slow and fast LPF respectively, is

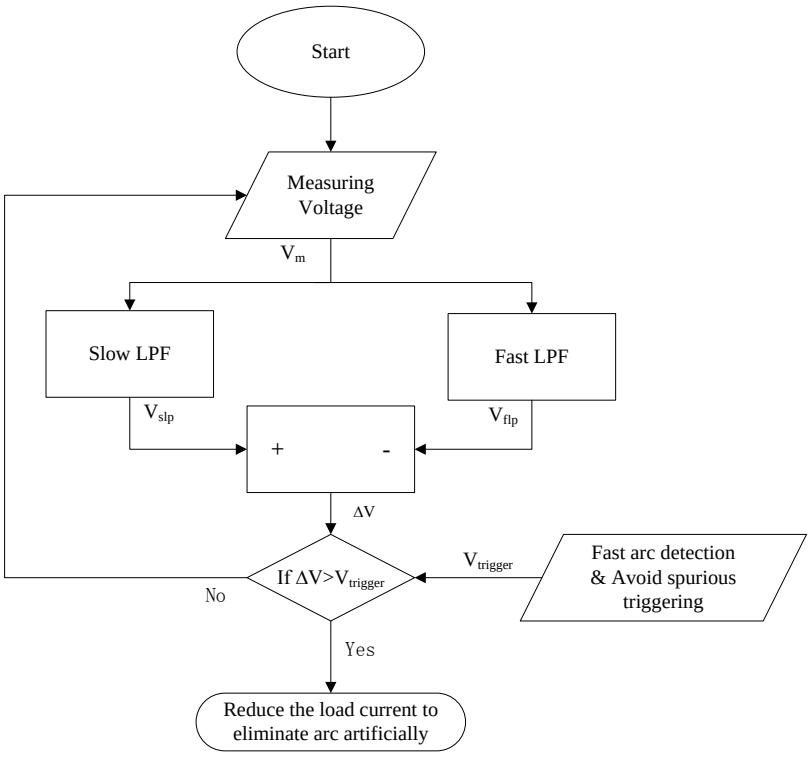

Figure 4-2: The arc detection algorithm based on drop in load voltage due to minimum electrode gap voltage of series dc arc [17].

greater than the setting value of the threshold voltage (V_{trigger}), it means that the arc inception is detected and the current controllable unite will be signalled to reduce the load current to zero at the appropriate rate to extinguished the series dc arc fault as soon as possible in order to avoid undesired damage.

$$\Delta V = V_{\text{slp}} - V_{\text{flp}} > V_{\text{trigger}} \tag{4-3}$$

Moreover, what is important to keep in mind is that the speed of the arc detection algorithm would be influenced by the selection of the threshold voltage value which should be determined by both the occurrence of actual electrode dependent load voltage drop and the avoidance of spurious triggering [17].

In theoretically, a low pass filter intends to imposes high attenuation above a specified frequency and little or no attenuation below that frequency. The frequency at which the transition occurs is called the cut-off frequency.

The function of the low pass filter circuit shows the frequency response of the filter to be

nearly flat for low frequencies and all of the input signal is passed directly to the output, resulting in a gain of nearly 1, until it reaches its cut-off frequency point (f_c) [17]. Moreover, any high frequency signals applied to the low pass filter circuit above this cut-off frequency point will attenuated.

It is known that the phase shift of the circuit lags behind that of the input signal due to the time required to charge and then discharge the capacitor as the sine wave changes. This combination of R and C produces a charging and discharging effect on the capacitor known as its time constant (τ) of the circuit. The time constant is related to the cut-off frequency (f_c) as:

$$\tau = \frac{1}{2\pi f_c} \tag{4-4}$$

The output voltage depends upon the time constant and the frequency of the input signal. With a signal inputting over time, the circuit behaves as a simple 1st order low pass filter with the functions as discussed above. Furthermore, the function of 1st order LPF can be expressed mathematically as:

$$G(s) = \frac{1}{Ts + 1} \tag{4-5}$$

with T equals to the value of time constant (τ) of LPF circuit.

Then by carefully selecting the correct time constant combination, a special filter circuit can be created that allows only a range of frequencies in a certain bandwidth value to get through the filter unaffected while any frequencies applied to the circuit out of these cut-off point to be attenuated, creating what is commonly called a band pass filter.

4-2 Modeling for the Equivalent Simulation System

In this section, the selectivity of the series arc detection and elimination algorithm is validated theoretically in MATLAB. A Simulink model is established with a typical representative dc micro-grids consisting of two constant power loads connected in parallel with arcing at DC-side of point of common coupling. Although a practical dc micro-grids can be more complicated with different kinds of variable renewable sources and energy storage devices, this equivalent dc circuit is adopted as a generic example to analyse the response and reaction of the proposed series dc arc detection method.

4-2-1 Equivalent Circuit

The diagram shown in Fig.4-3, is the equivalent circuit used in the model building which is used to validate the function of the proposed series dc arc detection and elimination algorithm which was discussed in Section.4.1.

The state space equations derived for the equivalent circuit are described below.

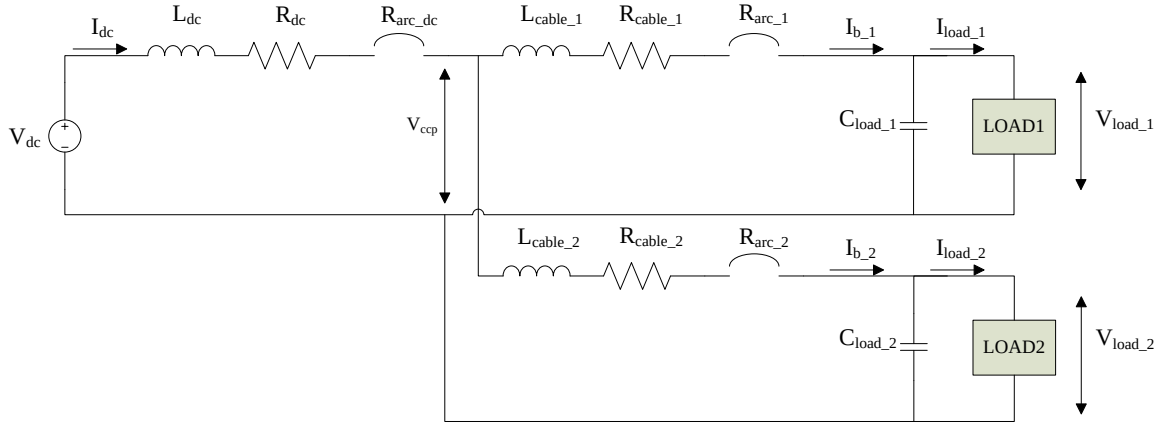

Figure 4-3: The equivalent circuit diagram for two parallel loads.

$$\frac{\mathrm{d}I_{\mathrm{dc}}}{\mathrm{d}t} = \frac{1}{L_{\mathrm{dc}}}(V_{\mathrm{dc}} - V_{\mathrm{ccp}} - (R_{\mathrm{arc\_}dc} + R_{\mathrm{dc}})I_{\mathrm{dc}}) \tag{4-6}$$

$$\frac{\mathrm{d}I_{\mathrm{b\_1}}}{\mathrm{d}t} = P_1 \cdot \frac{1}{L_{\mathrm{cable\_1}}}(V_{\mathrm{ccp}} - V_{\mathrm{load\_1}} - (R_{\mathrm{arc\_1}} + R_{\mathrm{cable\_1}})I_{\mathrm{b\_1}}) \tag{4-7}$$

$$\frac{\mathrm{d}V_{\mathrm{load\_1}}}{\mathrm{d}t} = \frac{1}{C_{\mathrm{load\_1}}}(I_{\mathrm{b\_1}} - I_{\mathrm{load\_1}}) \tag{4-8}$$

$$\frac{\mathrm{d}I_{\mathrm{b\_2}}}{\mathrm{d}t} = P_2 \cdot \frac{1}{L_{\mathrm{cable\_2}}}(V_{\mathrm{ccp}} - V_{\mathrm{load\_2}} - (R_{\mathrm{arc\_2}} + R_{\mathrm{cable\_2}})I_{\mathrm{b\_2}}) \tag{4-9}$$

$$\frac{\mathrm{d}V_{\mathrm{load\_2}}}{\mathrm{d}t} = \frac{1}{C_{\mathrm{load\_2}}}(I_{\mathrm{b\_2}} - I_{\mathrm{load\_2}}) \tag{4-10}$$

$$I_{\mathrm{dc}} = I_{\mathrm{b\_1}} + I_{\mathrm{b\_2}} \tag{4-11}$$

Based on (4-11), the voltage at the common coupling point (V_{ccp}) can be derived from (4-6),(4-7) and (4-9) as shown in (4-12).

$$V_{\mathrm{ccp}} = \frac{\left(\frac{V_{\mathrm{dc}}}{L_{\mathrm{dc}}} + P_1\frac{V_{\mathrm{load\_1}}}{L_{\mathrm{cable\_1}}} + P_2\frac{V_{\mathrm{load\_2}}}{L_{\mathrm{cable\_2}}}\right) - \left(\frac{I_{\mathrm{dc}}}{\tau_{\mathrm{dc}}} + P_1\frac{I_{\mathrm{b\_1}}}{\tau_{\mathrm{b\_1}}} + P_2\frac{I_{\mathrm{b\_2}}}{\tau_{\mathrm{b\_2}}}\right)}{\left(\frac{1}{L_{\mathrm{dc}}} + \frac{P_1}{L_{\mathrm{cable\_1}}} + \frac{P_2}{L_{\mathrm{cable\_2}}}\right)} \tag{4-12}$$

With the time constants $\tau_{\mathrm{dc}} = \frac{L_{\mathrm{dc}}}{R_{\mathrm{dc}}}$, $\tau_{\mathrm{b\_1}} = \frac{L_{\mathrm{cable\_1}}}{R_{\mathrm{cable\_1}} + R_{\mathrm{arc\_1}}}$ and $\tau_{\mathrm{b\_2}} = \frac{L_{\mathrm{cable\_2}}}{R_{\mathrm{cable\_2}} + R_{\mathrm{arc\_2}}}$.

where in case of constant power load (P_{load}), the load current should be calculated as 4-13.

$$I_{\text{load}} = \frac{P_{\text{load}}}{V_{\text{load}}} \tag{4-13}$$

In order to adjust the equivalent mathematical equations based on the real circuit to present the correct response to the change in the structure of the circuit, the modeling parameter P_1 and P_2 were set for branch 1 and branch 2 respectively in value of "1" when the corresponding branch connected to common coupling point which means that the branch with the load was attached to the whole system. While, when an arcing fault was introduced in the system, since the arc resistance is inversely proportional to the arc current, if the computed $R_{\text{arc}} > 100k\Omega$ and the measured arc current $< 1e^{-6}A$ (R_{arc} becomes infinity when I_{arc} goes to zero), the related branch is assumed to be disconnected to the system, and the corresponding modeling parameter is set to "0", which means that arc is stamped out in the circuit.

The equivalent circuit of DC micro-grids system has been translated into the modeling in Simulink which works on the mathematics relations derived as shown in the Equations from 4-6 to 4-12.

4-2-2 Equivalent Arc Resistance.

As mentioned in the Chapter 3, when building the model for arc, some important quantities should be taken into consideration, such as the electrode material, geometry of the electrode contactors, the speed of the contactors separation, the electrode gap length, the arc current and the voltage across the arc.

In order to accurately model the electrical behaviour of arcing, the series dc arc is treated as a variable resistance.

For the copper material electrode discussed in our modelling, the initial electrode material dependent arc voltage is $13.3V$ in the open air according to Table.4-1, the voltage variation with gap length and arc current is estimated based on the empirical equations for dynamically varying resistance

As explained in [22, 27], in the open air, if the arc current $I_{\text{arc}} < 100A$ in Low Voltage (LV) level networks, the empirical relations between different electrode gap lengths and arc resistance is shown in Table.4-2 to which according the series dc arc resistance can be represented by applying the linearly interpolation between the different known data points in sequence.

As a consequence, arcing during plug out can be simulated by input of a series resistance dependent on the arc length and arc current.

Table 4-2: Empirical Computation Equations for Arc Resistance.

Electrode Gap Length(mm)	Arc Resistance(Ω)
1	36.32 $I_{\text{arc}}^{-1.124}$
5	71.39 $I_{\text{arc}}^{-1.186}$
10	105.25 $I_{\text{arc}}^{-1.239}$
20	153.63 $I_{\text{arc}}^{-1.278}$
50	262.02 $I_{\text{arc}}^{-1.310}$
100	481.20 $I_{\text{arc}}^{-1.350}$
200	662.34 $I_{\text{arc}}^{-1.283}$

4-3 Simulation Results of the Detection Method

The proposed arc detection algorithm is simulated under the condition of two parallel constant power loads both in the value of $470W$ with the input capacitance of $30\mu F$ [28].

As the system parameters listed in Table.4-3, the equivalent circuit is energized with a dc source voltage (V_{load}) of $100V$. In grid side, $100\mu H$ and 0.25Ω are chosen as the value for inductance (L_{dc}) and the resistance (R_{dc}). While, load-side resistance (R_{cable}) and load-side inductance (L_{cable}) are set with the value of 0.01Ω and $3\mu H$ respectively for the two branches.

Table 4-3: Simulation Parameters for equivalent circuit.

Parameters	Symbol	Values
DC source voltage	V_{dc}	$100V$
DC-source side inductance	L_{dc}	$100\mu H$
DC-source side resistance	R_{dc}	0.25Ω
Load side inductance	L_{cable}	$3\mu H$
Load side resistance	R_{cable}	0.01Ω
Load capacitance	C_{load}	$30\mu F$
Constant power load	P_{load}	$470W$

During the simulation, in order to attenuate both the low frequency grid-side voltage fluctuation ($< 150Hz$) and the high frequency switching ripple of load-side power electronics components ($> 10kHz$), the value of time constant for slow LPF is in value of $0.001s$, while $0.0001s$ is chosen for the fast LPF [26], and the threshold voltage is set as $10V$.

Table 4-4: Detection Algorithm Parameters in Theoretical Simulation.

Parameters	Symbol	Values
Slow LPF time constant	τ_{s}	$1ms$
Fast LPF time constant	τ_{f}	$0.1ms$
Trigger Voltage	V_{trigger}	$10V$

Fig.4-4 illustrates that the voltage response of the series dc arc detection algorithm in the simulation to the arcing initiation at the dc side by introducing arc current and length dependent resistance. Since the band pass filter with different time constant values shows different response, the output voltage from Slow LPF and Fast LPF shows different dropping speed. As a result, the voltage difference associated with the initial arc voltage drop reaches the trigger voltage value in $0.2ms$ after the arc initiation at the moment of $1ms$ by the arc detection methods at both the load1 and load2 side, which represents that the series dc arc at dc side is detected by the converter at load side with high selectivity and speed guaranteed.

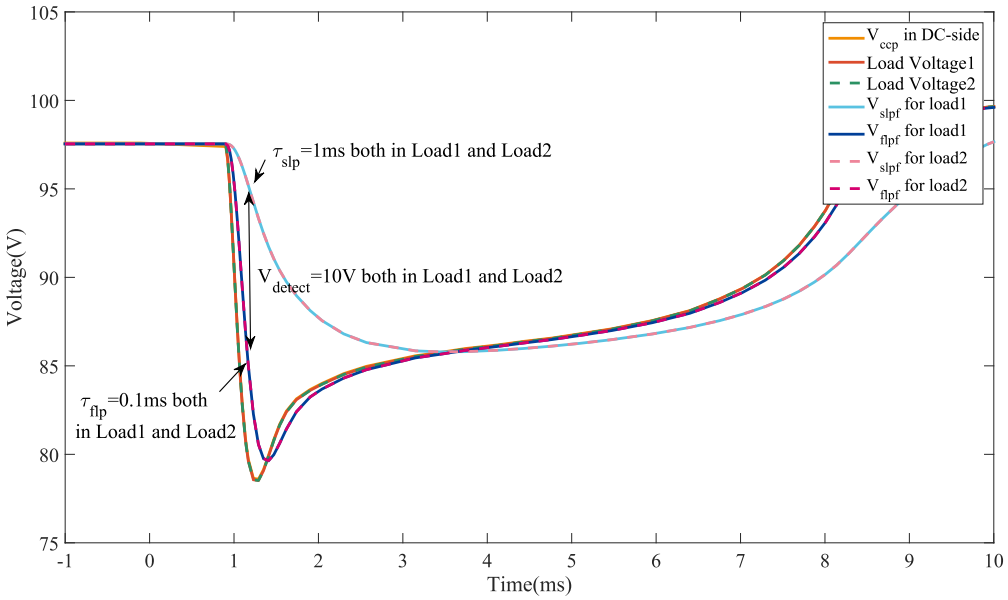

Figure 4-4: The simulated voltage response for arc fault at DC-side with arc detection and elimination algorithm.

According to the current response which can be observed from Fig.4-5, with load voltage

decreasing, the load current increases to obtain the constant power for the load. When the arc detection signal from the detection algorithm is triggered, both the $I_{\text{load\_1}}$ and the $I_{\text{load\_2}}$ are ramped at $-0.7A/ms$ at the same time. Within $7ms$ after arc initiation, I_{dc} reaches zero and hence arc at dc side was quenched entirely by lowering the current in both load1 and load2 side at the appropriate speed considering the constrains of the dc micro-grids system and the arcing damage.

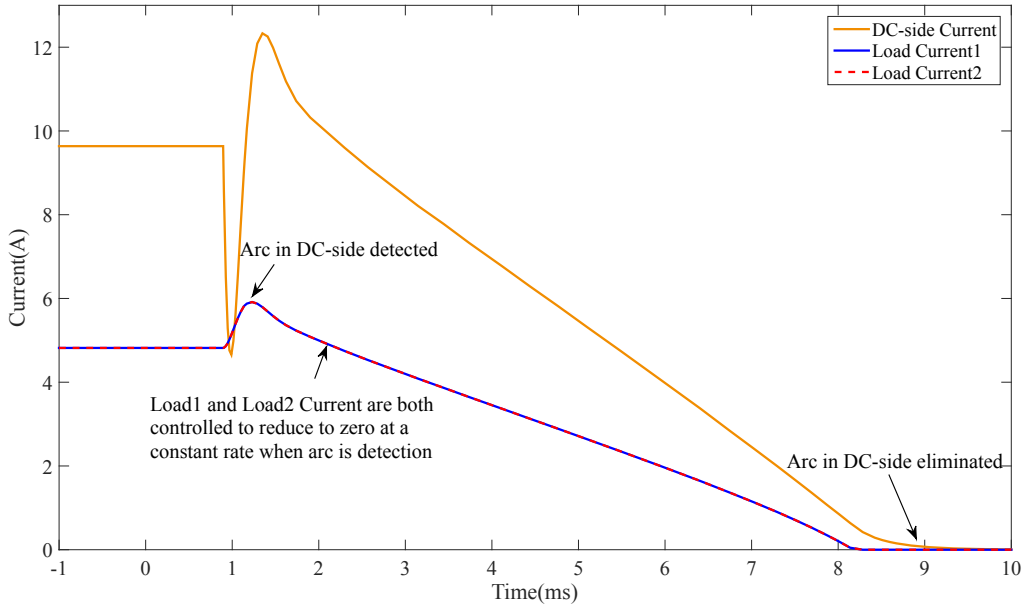

Figure 4-5: The simulated current response for arc fault at DC-side with arc detection and elimination algorithm.

4-4 Conclusion

In this Chapter, the selectivity and rapidity of the proposed series dc arc detection algorithm has been theoretically validated through modeling in MATLAB, especially when the series dc arc fault initiated at dc side in the dc circuit connected with two parallel constant power loads with input capacitance with the ability to localize arcing fault.

Chapter 5

DC Series Arc Characterization and Influencing Factors

The theoretical validation of the arc detection algorithm has been performed in previous chapter. In this chapter, the factors influencing the characteristics of series dc arc behaviour are studied, such as the dc source voltage, the load current, the grid inductance and the load input capacitance, which would be used to the determine the parameters of the proposed series dc arc detection algorithm.

Since the theory of the series dc arc detection algorithm emulated in this thesis is based on the load-side voltage drop caused by the initial arc voltage at the arc inception, it is useful to investigate the arc behaviour, like the arc generation, arc sustainability, the initial arc voltage drop and the related time.

5-1 Setup for the Experiment

The system shown in Fig.5-1 is analysed the influencing factors of the circuit on the arc behaviour. And the series dc arc can be created by switching the relay off the energized circuit.

The electric arc behaviour is determined by the electrode materials, arc current, gap length and contact separation speed.

As shown in Fig.5-1, a series RLC circuit acts as a low pass filter for the load side voltage across the capacitor, the high frequency components of the injected arc voltage are bypassed. As discussed in [28], the magnitude of gird inductance, resistance and capacitance will influence the load-side voltage drop in response to the series arc both in terms of peak value and

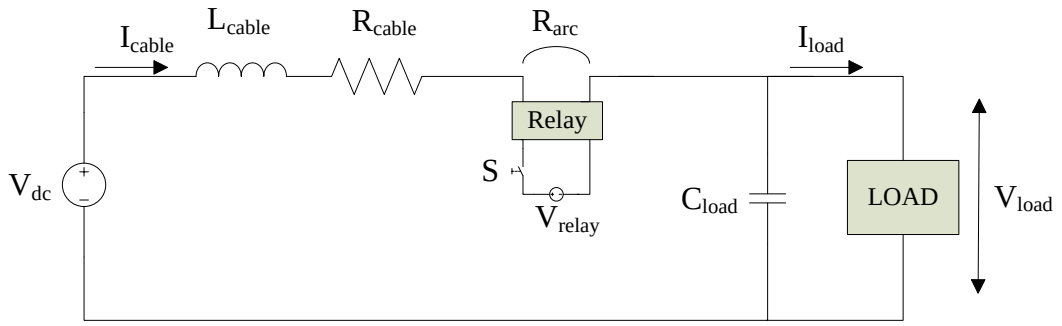

Figure 5-1: The equivalent circuit diagram for arc behaviour experiments.

the rise time. The empirical understanding of the influencing factors is required to set the threshold voltage of the detection algorithm, and also to understand if and when sustained series arcs occur in dc microgrids

The Table.5-1 summarizes the test setup parameters for the series arc behaviour tests.

Table 5-1: Experiment Parameters for Arc Behaviour Test.

Parameters	Symbol	Values
DC source voltage	V_{dc}	$48V$, $75V$, $100V$
Cable resistance	R_{cable}	0.01Ω
Cable inductance	L_{cable}	$100\mu H$, $150\mu H$, $200\mu H$
Load capacitance	C_{load}	$0\mu F$, $17\mu F$, $27\mu F$
Load current	I_{load}	$3A$, $4A$, $5A$
Number of each test	n	6

In order to examine the influence of dc source voltage and load current on the characteristics of series dc arc, tests under both changing voltage and current tests were carried out. The experimental procedure was conducted as follows:

At first, the dc source voltage is set at $48V$ and the load current is set to be $3A$, $4A$ and $5A$ by adjusting the resistive load. Then, the dc source voltage is increased to $75V$ and the above these load current levels are adjusted again successively. The same procedure is repeated for dc source voltage of $100V$.

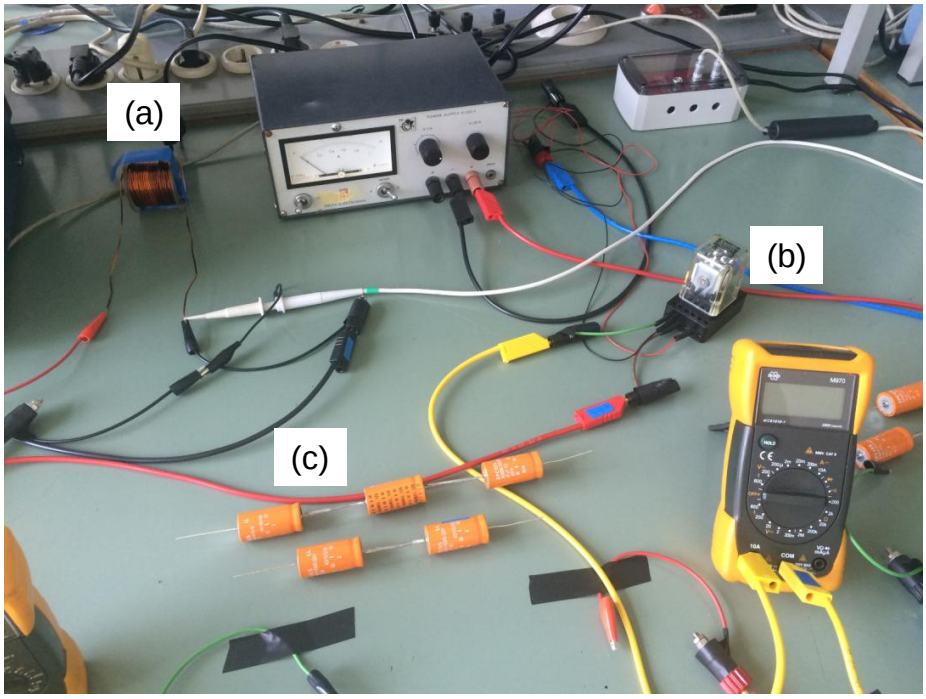

Figure 5-2: The practical setup for series dc electric arcing study, (a) Grid Inductance, (b) Arcing Relay, (c) Load Capacitance.

Meanwhile, aiming to investigate the influence of the grid inductance and load input capacitance on the characteristics of arc, load side voltage drop and the time needed to reach this value are measured directly under the following different conditions: grid inductance (L_{cable}) of $100\mu H$, $150\mu H$, $200\mu H$, while load capacitance (C_{load}) of $0\mu F$, $17\mu F$, $27\mu F$ with the procedure described in above paragraph repeated for each variable changes. And experiment under similar parameter condition is repeatedly conducted with six times to gain statistical understanding of the stochastic series arcing process.

All of the measurement signals, including load side voltage and arc current were recorded by using the YOKOGAWA DLM2054 mixed signal oscilloscope 2.5GS/s 500MHz. This oscilloscope has an analog to digital conversion resolution of 16 bits and the sampling rate used for the test is 6.25MS/s. Both the onset of the arc and the stable arcing were recorded.

The experimental setup has been built as shown in Fig.5-2 with arcing relay, grid inductance and load capacitance.

5-2 Impact on the Arc Generation and Sustainability

As shown in Fig.5-3(a) to Fig.5-3(c), the categories of the arcing have been displayed. Fig.5-3(a) means arcing occurs but sustains for a long time, while Fig.5-3(b) displays the situation of no arcing with current drops instantaneously to zero. Sustainable arcing is shown in Fig.5-3(c) with an initial voltage drop and decreases in a gradient due to increasing arc gap length.

Next, by varying the value of circuit parameters, the influencing factor would be explained in details below.

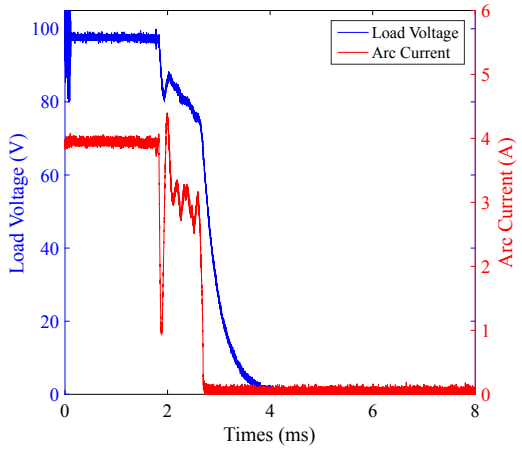

(a) Un-Sustainable Arcing

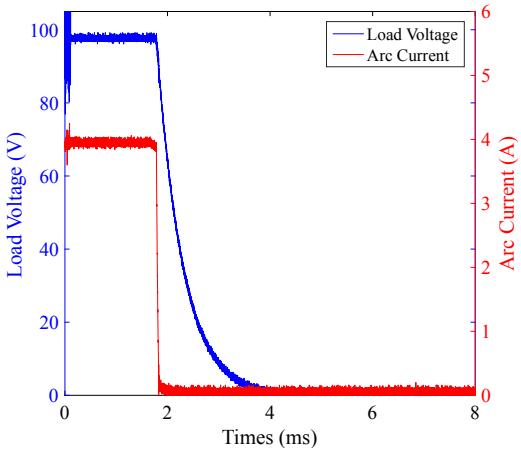

(b) No Arcing

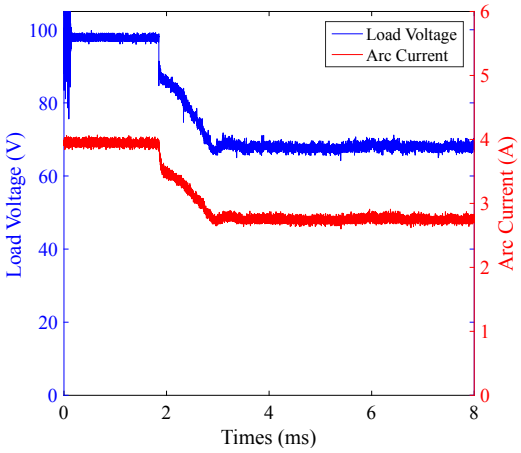

(c) Sustainable Arcing

Figure 5-3: The different categories of series dc arc.

5-2-1 DC Source Voltage and Load Current

The arc generation probability distribution plot is shown in Fig.5-4. The number in the plot represents the probability of the number of adequate tests over the total number of the tests with different value of load voltage, load current, load capacitance and dc-side inductance which were displayed as four arguments in the probability distribution plot.

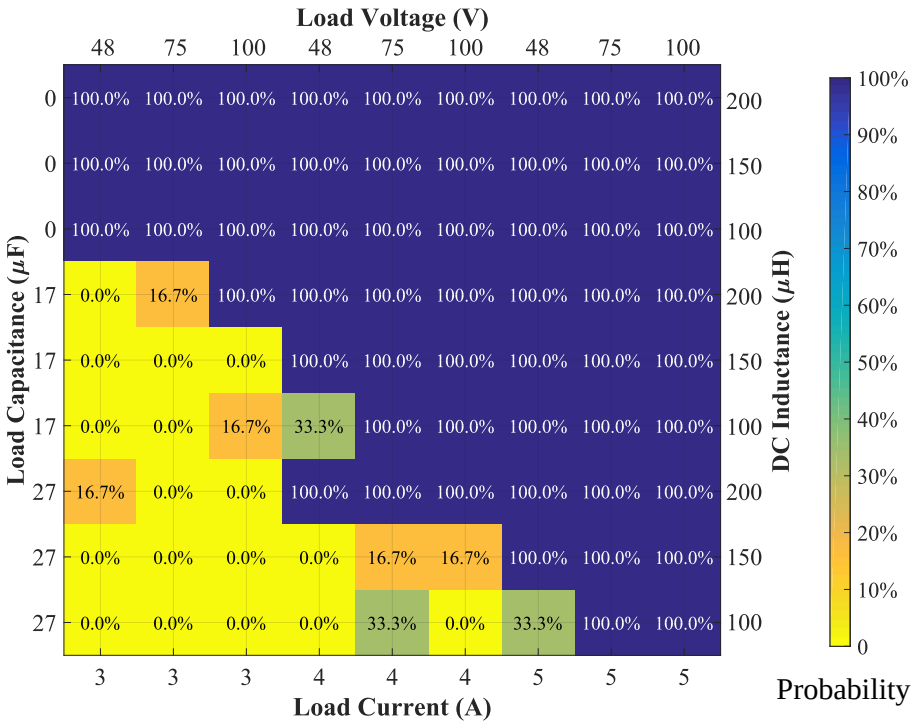

Figure 5-4: The probability distribution of arc generation.

First, the influence of dc source voltage and load current would be discussed in this section. As mentioned in the Chapter 3, Fig.3-1 [18] illustrates the generation of an arcing due to the separation of electrode contactor, with the relay electrode contactor being forced to separate instantaneously and the current density increasing significantly, the heat generated at the contactor spots begins to increase dramatically, which results in the melting of metal and generating metallic evaporation.

Increasing current increases the energy input to the arc with higher current density, thereby, increasing the probabilities of arc generation.

From the Fig.5-4 in which the information about the situation of arcing with different circuit parameters is shown, the higher load current increases the probability of series dc arc generation.

It can be observed that the arcing generation probability increases from 0% to 33.3% and then to 100% with increasing value of I_{load} ($3A$, $4A$ and $5A$), when the circuit parameters chosen as $V_{\text{load}} = 48V$, $L_{\text{cable}} = 100\mu H$ and $C_{\text{load}} = 17\mu F$.

While, in the condition of $I_{\text{load}} = 3A$, $L_{\text{cable}} = 200\mu H$ and $C_{\text{load}} = 17\mu F$, the arcing probability is 0%, 16.7% and 100% respectively when the V_{load} is set to be $48V$, $75V$ and $100V$. However, in the condition of $I_{\text{load}} = 4A$, $L_{\text{cable}} = 100\mu H$ and $C_{\text{load}} = 27\mu F$, arc occurs only when V_{load} equals to $75V$, which indicates that the voltage level has minimal impact on the probability of arc generation.

Meanwhile, the Fig.5-5 and Fig.5-6 shows the probability distribution of sustainable arc and the arc burning time respectively among different parameters in tests.

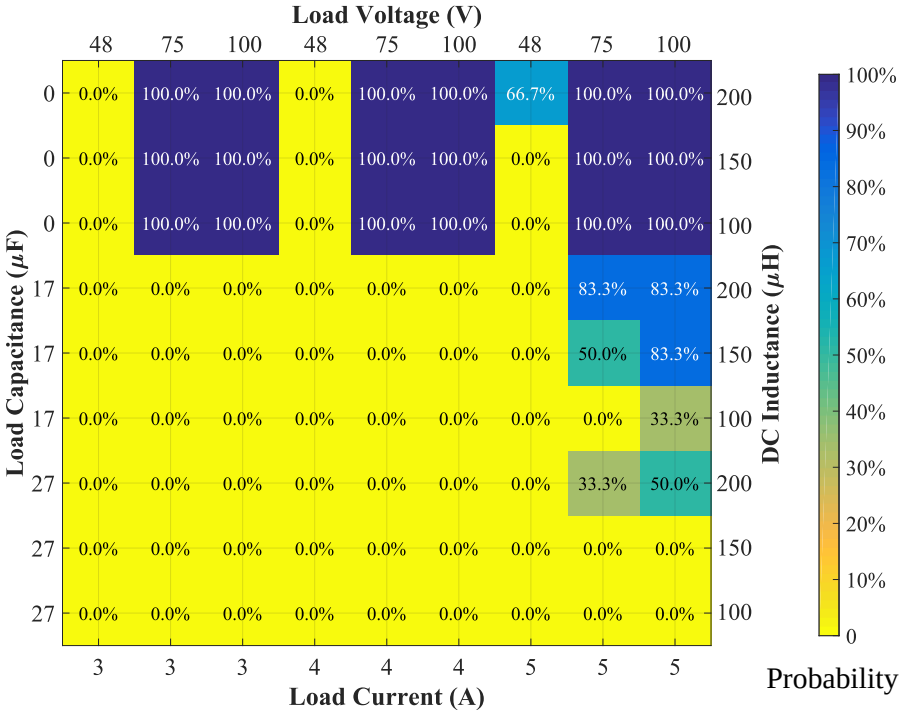

Figure 5-5: The probability distribution of arc sustainability.

What can be easily observed is that when the value of load-side input capacitance (C_{load}) becomes zero, the series dc arc would be sustainable when the dc voltage is equal and higher than $75V$. More convincing results about the impact of V_{load} on the arcing sustainability laid in the condition of $I_{\text{load}} = 5A$, $L_{\text{cable}} = 150\mu H$ and $C_{\text{load}} = 17\mu F$ with 0%, 50% and 83.3% in probability and $1.49ms$, $3.67ms$ and $15.09ms$ in average arc burning time for different and V_{load} ($48V$, $75V$ and $100V$).

Furthermore, in case of $V_{\text{load}} = 48V$, $L_{\text{cable}} = 200\mu H$ and $C_{\text{load}} = 0\mu F$, when the I_{load} reaches $5A$, the probability is 66.7% different from 0% for $3A$ and $4A$, which shows that with increasing the value of load current, both the probability of sustainable arc and the average time of arc burning increase.

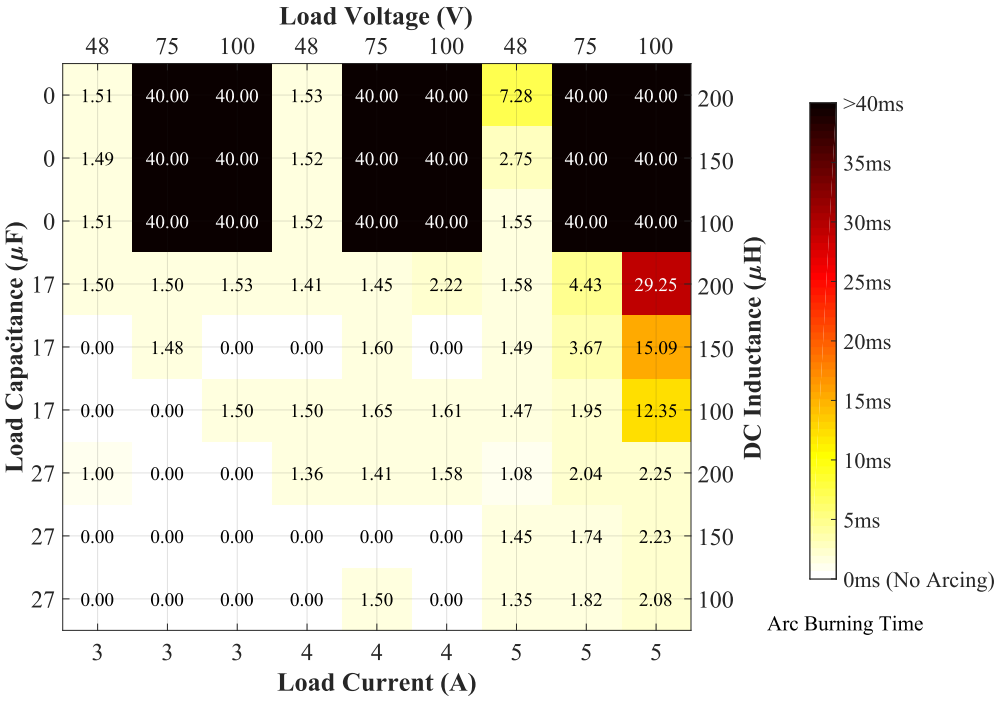

Figure 5-6: The arc burning time under different circuit conditions.

5-2-2 Grid Inductance and Load Input Capacitance

By analysing the three rows of results in the bottom of the Fig.5-4 ($V_{\text{load}} = 100V$, $I_{\text{load}} = 4A$, and $C_{\text{load}} = 27\mu F$), the inductance shows an effect on the arc generation (with 0%, 16.7% and 100% in probability for $100\mu H$,$150\mu H$ and $200\mu H$) due to the inductance will force the current to flow and hold the current to avoid changing, which results in the variation in the value of load current changes slowly and then the electrode contactor have enough time to evaporate the metal in the material of copper to create an arc.

As for the sustainability of the series dc arc in respect of average arc burning time, from the Fig.5-5 and Fig.5-6, especially when load current equals to $5A$, voltage equals to $100V$ and capacitance is $17\mu F$, with raising the value of the inductance from $100\mu H$ to $200\mu H$, the probability of arc sustainability presents a rising trend from 0% to 50% and to 83.3% in probability and $12.35ms$, $15.09ms$ and $29.25ms$ in average arc burning time.

Since the capacitance in parallel with the load holds the inherent capability to keep the load voltage (V_{load}) from changing instantly, the voltage across the electrode contactor gap cannot vary immediately to satisfy the requirement of arc initiation due to the current density on the electrode contactor is too weak to melt the metal into the ionized particles to form plasma channel bridging the gap, which results in the decreasing of probability on arc generation.

With increasing the value of the capacitance from top to bottom in the Fig.5-4, the probability of arc generation decreases.

The larger the value of the capacitance, the larger the capability of the capacitor to hold the certain value of the voltage. However if the voltage level is too enough to be held from changing by the capacitor, as a result, the voltage across the capacitor would change and then the voltage over arc will reach the minimal value to trigger the generation process of an arcing.

As well, the capacitance presents the same impact on the arc sustainability as the one on the arc generation, Fig.5-5 and Fig.5-6 illustrate that when the value of capacitance set to be zero, the probability of arc sustainability can reach the 100%, moreover the series dc arc can burn longer than $40ms$. When observing the results under the condition of $V_{\text{load}} = 100V$, $I_{\text{load}} = 5A$, and $I_{\text{cable}} = 200\mu H$, with choosing the capacitance in the value of $0\mu F$, $17\mu F$ and $27\mu F$, the probability responses in 100%, 83.30% and 50% respectively, while the average arc burning time decreases from $> 40ms$ to $29.25ms$ and then to $2.25ms$. As a consequence, it can be concluded that lowering the capacitance value will increase the probability of arc obtaining sustained series arcs.

5-3 Impact on the Load Voltage Drop and Time Delay

Following the discussion of the generation and sustainability of arcing, the research to study the influence of the circuit parameters on the characteristic of load voltage due to the series arc injection is important, because the load voltage variation is the critical foundation value in the proposed series dc arc detection method in this thesis.

The plots of the average drop value of the load side voltage and the average drop time with error-bar caused by the arc inception under six tests for each different circuit parameters are given in Fig.5-7 and Fig.5-8.

5-3-1 DC Source Voltage and Load Current

In Fig.5-7, by comparing the three subplots under different value of dc source voltage ($48V$, $75V$ and $100V$), the external dc source voltage shows a negligible influence on the load side voltage drop caused by the arc injection under the same condition including the load current, grid inductance and load capacitance. Though a statistical variation in load voltage is

observed due to stochastic nature of electric arcs, no clear trend is observed with varying dc source voltage.

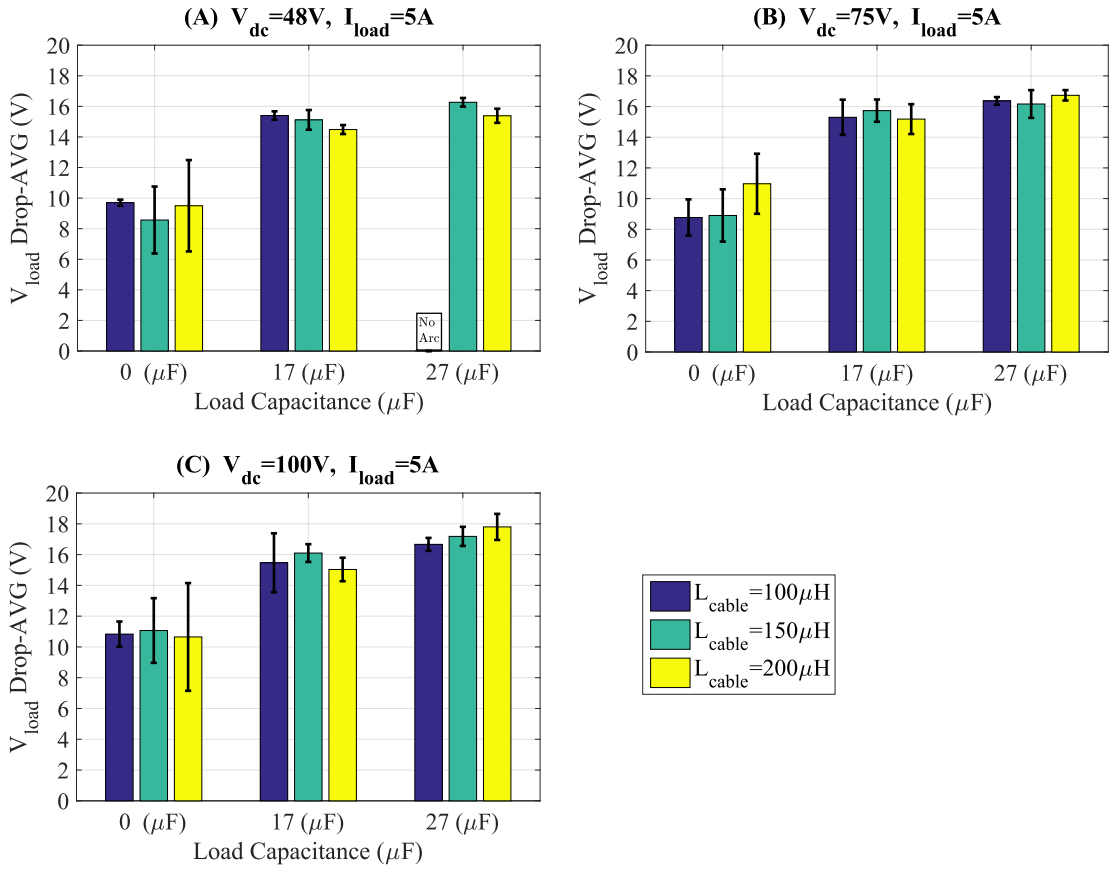

Figure 5-7: The initial load voltage drop under different circuit parameters.

The same result appears in the average drop time as shown in the Fig.5-8, the dc source voltage value leads to no clear impact on the value of the time delay for load side voltage to reach the initial value caused by the arcing injection.

While, under different circuit parameters, it can be analysed that load current has a slight influence on the drop value of the load voltage.

As for the time delay, apparently, there is no impact on it caused by changing the value of load current.

5-3-2 Grid Inductance and Load Input Capacitance

By analysing the results as shown in the Fig.5-7 and Fig.5-8, the grid inductance and load side capacitance values pose the influence not only on the magnitude of the load voltage drop

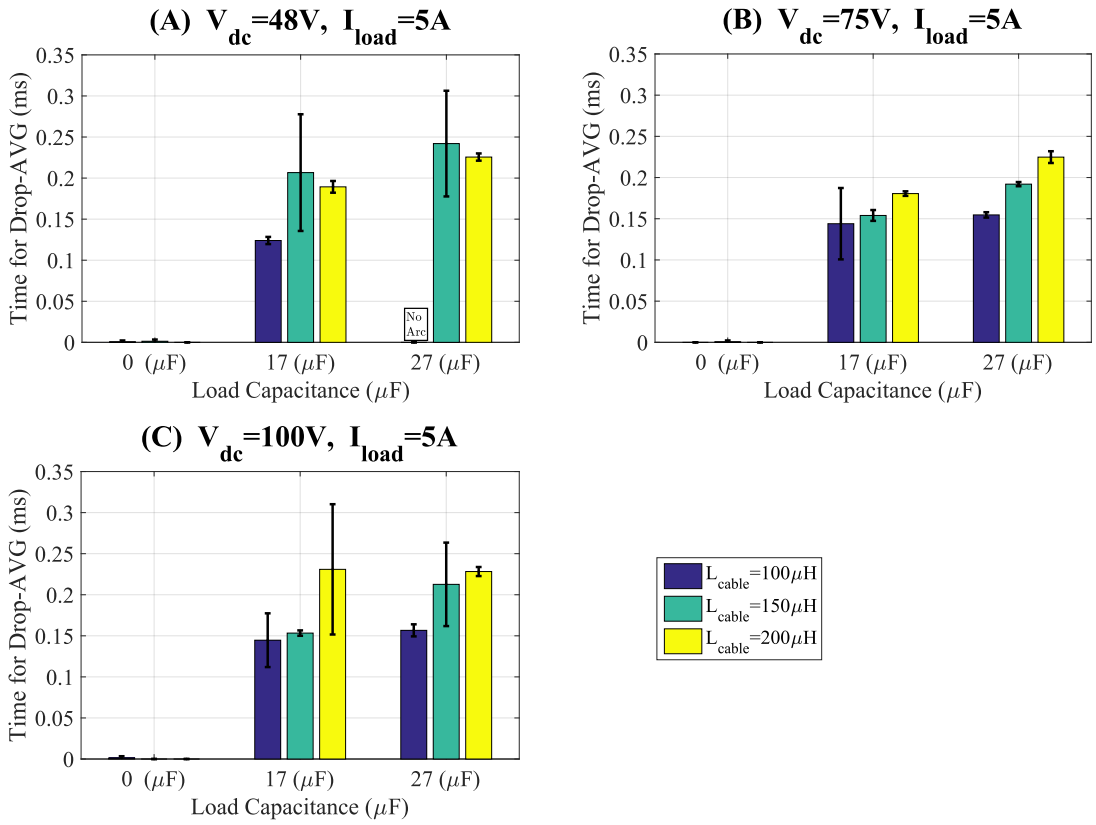

Figure 5-8: The initial load voltage drop time under different circuit parameters.

but also on the time needed to reach the detection threshold value when the arc occurs, which should be taken into consideration in the designing of the series dc arc detection algorithm.

The Resistance, Inductance and Capacitance (RLC) act as a low pass filter circuit for the load voltage. As a consequence of the series resonance between inductance and capacitance, the magnitude response of the load side voltage to input voltage can be calculated by 5-1 [17]. While, the frequency of input voltage is $\omega = 2\pi f$, and the natural frequency of the LPF is $\omega_0 = 2\pi f_0$ and the quality factor Q is $\frac{\omega_0}{\alpha}$ ($\alpha = \frac{R}{2L}$).

$$\frac{|V_c|}{|V_i|} = \frac{1}{\sqrt{\left(1 - \left(\frac{\omega}{\omega_0}\right)^2\right)^2 + \left(\frac{\omega}{Q\omega_0}\right)^2}} \tag{5-1}$$

What can be found in Fig.5-9 [17] is that, with increasing the value of quality factor($Q = \frac{1}{R}\sqrt{\frac{L}{C}}$), when the natural frequency is close to the frequency components of the arcing voltage and then the Q is larger than unit 1, as a result, the initial load voltage drop measured at

the load side increases to the value greater than the initial arc voltage due to the arc inception.

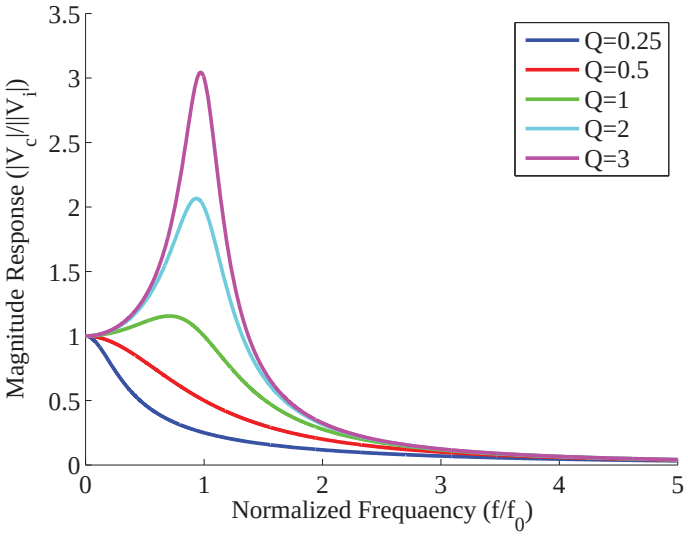

Figure 5-9: The magnitude response of load side voltage for different quality factor values.

Now paying an attention on the effect of capacitance on the experiment results which has been summarized in Fig.5-7:

- With increasing the value of capacitance for the same resistance and inductance from $0\mu F$ to $17\mu F$, there appears a R-L-C low pass filter circuit, and the quality factor (Q) of the experiment circuit is greater than 1, which causes that the initial drop of the load voltage measured across the capacitor (around $15V$) become higher than the initial arcing voltage drop (around $10V$ when $C_{\text{load}} = 0\mu F$) independent of the voltage and the current.

- Furthermore, with the value of load input capacitor increasing from $17\mu F$ to $27\mu F$, the quality factor decreases according to the Equation($Q = \frac{1}{R}\sqrt{\frac{L}{C}}$), the load voltage drop should be lower. However the measured load voltage drop across the capacitance ($27\mu F$) shows higher value than the one at $C_{\text{load}} = 17\mu F$, with the magnitude of the detected voltage across the capacitance increases from $15V$ to $17V$. which is counter to the notion predicted as mentioned in [28].

  In the experiment, the dc source has a capacitance which is in series with load capacitance, and the net capacitance may be decreased. Meanwhile, instead of a constant step in simulation, the real arcing is created in tests, and the real process is not as similar as a constant step in voltage drop due to the introduction of capacitance at load side. The precious reason need to be investigated deeply in future.

As for the time for load voltage drop, the existence of load capacitance results in the load side output voltage lagging behind that of the initial voltage drop across the arcing resistance. Fig.5-8 displays that there are average $0.17ms$ and $0.23ms$ time delay being introduced in the series dc arc generation with increasing the capacitance value from $17\mu F$ to $27\mu F$. When the load input capacitance is absent in the circuit, from the Fig.5-8, it can be found that there is no time delay occurs and the load voltage drops to the initial value instantaneously.

The influence of grid inductance on the load voltage drop value is discussed as what is followed by:

- Seen from the Fig.5-7, the inductance shows negligible impact on the voltage drop under different dc voltage source when $C_{\text{load}} = 0\mu F$, and the drop value is around $9ms$ with a little variation for different inductance.
- When the capacitance becomes larger than zero, by increasing inductance and resistance for the same dc source voltage and load capacitance, the quality factor of the R-L-C resonance circuit decreases due to the dominant increase in the value of resistance which is inversely proportional against a direct square proportionality to inductance, which should result in the reduction in the load side voltage drop due to the lower quality factor as shown in Fig.5-7 (A).

  However, as a consequence of the introduction of capacitance, the complex results appears in Fig.5-7 (B) and (C), the average load voltage drop shows no trend under the increasing inductance which is not consistent with what is predicted in [28]. As explained for the impact of capacitance on the load voltage drop, during the experiments, there were the parasitic resistance still existing in the circuit, which will impact the total value of resistance in the quality factor calculation. And in the real inductor design, the real value of inductance and resistance may not be consistent with the theoretical values. To explain this phenomena in details, more research need to be conducted to investigate the reason behind the experiment results.

In the Fig.5-8, the impact of grid inductance on the load voltage drop time can be observed:

- When $C_{\text{load}} = 0\mu F$, the drop time is always zero under different value of grid inductance.
- While when the capacitance increasing from $0\mu F$ to $17\mu F$, it can be found that the rising inductance will increase the drop time especially under $V_{\text{dc}} = 75V$ and $100V$, due to the effect of resonance period in R-L-C circuit with the $T = 2\pi\sqrt{LC}$ in which the time period increases with larger inductance for the same value of capacitance.
- The same tendency appears for changing the grid inductance the with $C_{\text{load}} = 27\mu F$ under different dc source voltage.

The experiment results is consistent with the content about the initial arc voltage which has been discussed in Chapter 3, which would solidify the practical foundation for the series dc arc detection algorithm validated in this thesis.

5-4 Conclusion

This chapter mainly focuses on the influencing factors including dc source voltage, load current, grid inductance and load-side input capacitance on the arc behavior, mainly on the arc generation , the arc sustainability with burning time, the initial load voltage drop and the time required, which is essential and critical in the determination of the threshold voltage value of the series dc arc detection algorithm to achieve the accurate sensitivity and selectivity.

Chapter 6

Real- time Experimental Validation of Arc Detection Algorithm

The theoretical validation of arc detection algorithm and the arc behaviour research have already performed in previous part of the thesis. While, in this Chapter, the test setup is designed to conduct the experimental validation of sensitivity and selectivity of the series dc arc detection algorithm.

6-1 Real-time Arc Detection Test

In order to validate the proposed arc detection method, arcs were created in the experimental setup and voltage across the load was measured.

The typical experimental setup for real time arc detection is prepared according to the equivalent electrical circuit diagram shown in Fig.6-1.

During the experiment, a switch is used to control the arc generating relay to initiate an arcing in the circuit.

As for the realization of the arc detection, the detection algorithm has been embedded in micro-controller (LAUNCHXL-F28027F C2000 Piccolo LaunchPad Experimenter Kit), It is equipped by the same computing capability with the power electronic converter which is widely applied in the dc micro-grid system to analyse the electrical quantities and to control current and voltage eventually.

Because the maximum input voltage for the micro-controller is limited within $3.3V$, the

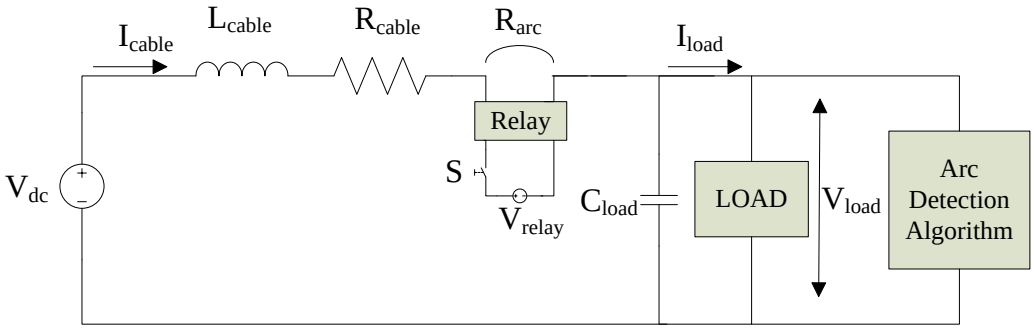

Figure 6-1: The equivalent circuit diagram for series loads with arc detection algorithm.

voltage divider(Appendix) is needed to convert the measured real-time load side voltage into the real-time micro-controller input voltage to meet the requirement of the security of the micro-controller operation.

In Fig.6-2, the interconnection between the voltage divider and the C2000 micro-controller is shown that: through a voltage divider with a constant ratio at $100/3.3V$, the load side voltage (V_{load}) can been modulated into the lower voltage ($V_{\text{out\_VD}}$) which can be fed into the micro-controller, and the real time measuring voltage value ($V_{\text{in\_analog}} = V_{\text{out\_VD}}$) should be translated from analog quantity data type into digital quantity data type ($V_{\text{in\_digital}}$) in order to be analysed in the micro-controller, while the Pin 'ADCINA0' of the micro-controller can automatically achieve that data type conversion.

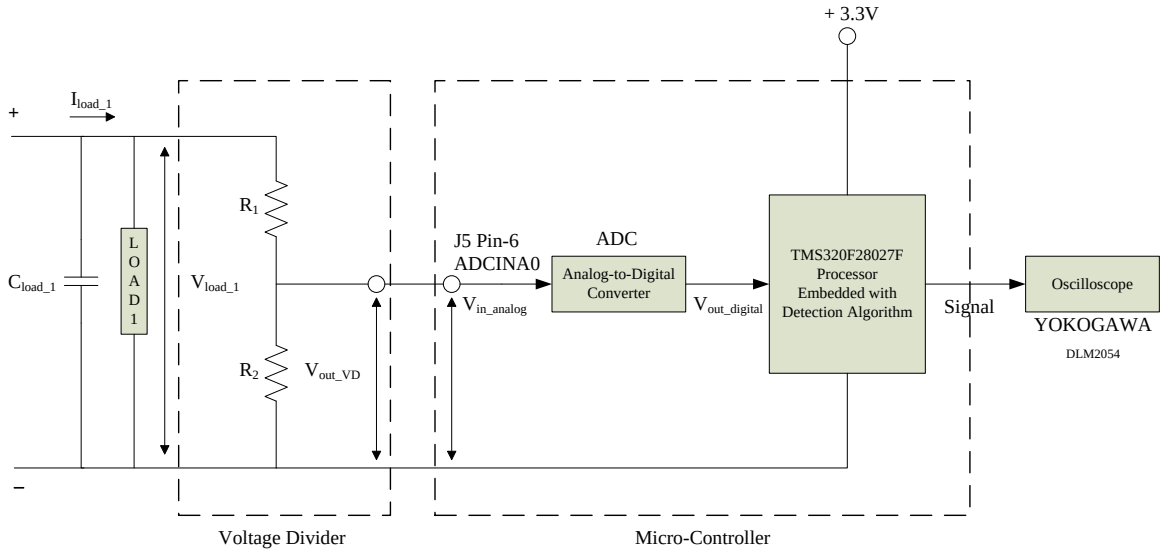

Figure 6-2: The connection diagram for micro-controller.

The detection algorithm theory used here is same as what has been stated in Chapter 4, a discrete band pass filter could let frequencies between 150-1500Hz pass through as a bandwidth of a slow LPF and a cascaded fast LPF with different time constant value.

However the micro-controller only adapt the discrete processing algorithm. The discrete time realization for the use in micro-controllers is given by 6-1, wherein, the smoothing factor α is computed based on the sample time ΔV and the required time constant of low pass filter as shown in the 6-2.

$$V_{\mathrm{lpf,k}} = (1-\alpha)V_{\mathrm{lpf,k-1}} + \alpha V_{\mathrm{load,k}} \tag{6-1}$$

$$\alpha = \frac{\Delta T}{\tau_{\mathrm{lpf}} + \Delta T} \tag{6-2}$$

6-2 Programming in Micro-controller

In order to make the activity of programming in micro-controller more efficiently, the coding of the arc detection algorithm was accomplished in MATLAB Simulink. Furthermore, the interconnection configuration between the MATLAB (R2015b) and the Code Composer Studio (V6.0.0) has been constructed step by step to facilitate the information exchange (Appendix B-2), and then the simulation programme designed in the MATLAB Simulink would be compiled into files in C language and burned directly into the micro-controller via a USB cable, which can help the engineers to achieve the convenient algorithm conversion from MATLAB Simulink blocks to Micro-controller processor.

It is worthy to be noted during the construction of Simulink block that the determination of the value of sample time set in both the micro-controller and the programme would have significant influence on the achievement of the series dc arc detection algorithm in the practical operation in the real world, because the sample time refers to the rate at which a discrete system samples the inputs and outputs. In case of these serial experiments, the sample time should be carefully chosen, and the value close to the lower time constant which is set for the Fast LPF could activate the functionalities of the arc detection algorithm in the micro-controller.

In the process of programming in the MATLAB Simulink, as shown in the Fig.6-2, the real measured load side voltage across the capacitance goes through the voltage divider, which presents the first transformation ratio. Furthermore, the second transformation ratio appears during the data type conversion from analog quantity to digital quantity occurs in the voltage value between input and output of the Pin ‘ADCINA0’ in the micro-controller of C2000.

In order to achieve the correct response of the arc detection algorithm in the micro-controller

with sensitivity, selectivity and speed, attention should be paid on the fact that the practical transformation ratio of both the voltage divider and the data type conversion posed a direct influence on the decision of settings of the arc detection method during the algorithm coding in the micro-controller.

When the output of band pass filter is greater than the set threshold value, a detection signal would jump from low voltage level to high voltage level, and be provided by the output pin 'GPIO3' from micro-controller to the oscilloscope which can be used to trigger the protection algorithm to shut down the load current.

6-3 Test on Sensitivity

The sensitivity for the arc detection algorithm will be studied experimentally under different circuit conditions with varying the trigger voltage value of the detection algorithm.

6-3-1 Setup and Procedure

The experimental setup for sensitivity test was prepared as what the Fig.6-3 presents according to the equivalent circuit shown in Fig.6-1.

Table 6-1: Experiment Parameters for Sensitivity Test.

Parameters	Symbol	Values
DC source voltage	V_{dc}	$100V$
Cable inductance	L_{cable}	$100\mu H$, $150\mu H$, $200\mu H$
Load capacitance	C_{load}	$0\mu F$, $17\mu F$, $27\mu F$
Load current	I_{load}	$5A$
Constant resistance load	R_{load}	Adjustable
Number of each test	n	5

Table 6-2: Detection Algorithm Parameters for Sensitivity Tests [28].

Parameters	Symbol	Values
Slow LPF time constant	τ_{s}	$1ms$
Cascading Fast LPF time constant	τ_{f}	$0.1ms$
Trigger Voltage	V_{trigger}	$6V$, $7V$, $8V$, $9V$

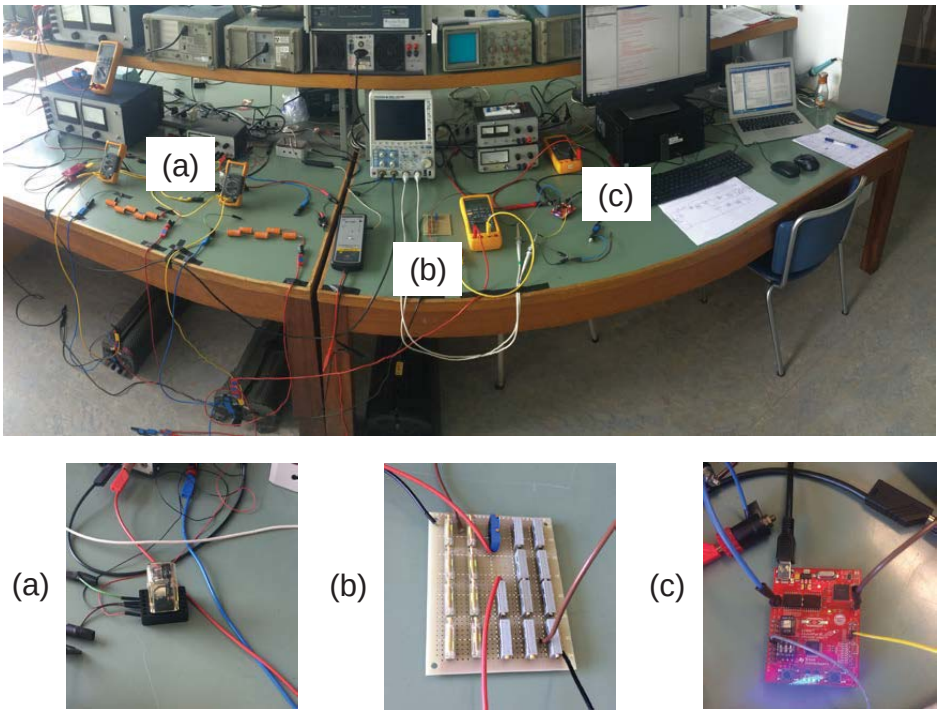

Figure 6-3: The practical setup with micro-controller for Sensitivity test, (a) Arcing Relay, (b) Voltage Divider, (c) Micro-Controller.

And the information of components associated with the experiment and the detection algorithm parameters [28] are summarized in Table.6-1 and Table.6-2 for arc detection sensitivity tests.

It can been seen that the dc voltage source supplies constant voltage value to the circuit, and the capacitance is connected to the constant resistance load in parallel. In order to study the sensitivity of the detection algorithm under different circuit parameters condition, not only grid inductance and load capacitance are varied, but also the trigger voltage is set at four different values. Each condition was repeatedly tested for five times to gain statistical insight about the stochastic arcing process.

To check the experiment result directly, the load side voltage and the arc detection signal from the micro-controller are recorded by oscilloscope (YOKOGAWA DLM2054 mixed signal 2.5GS/s 500MHz) to verify the functionality of the series dc arc detection algorithm.

6-3-2 Analysis of Experiment Results

For the set of experiments conducted with the same circuit parameters, as the threshold voltage detection value is increased from $6V$ to $9V$, Fig.6-4(a) to 6-4(d) present the different response of the detection algorithm to the varying trigger voltage value. With raising the value of the trigger voltage, the arc detection time increases, however the detection pitch decreases.

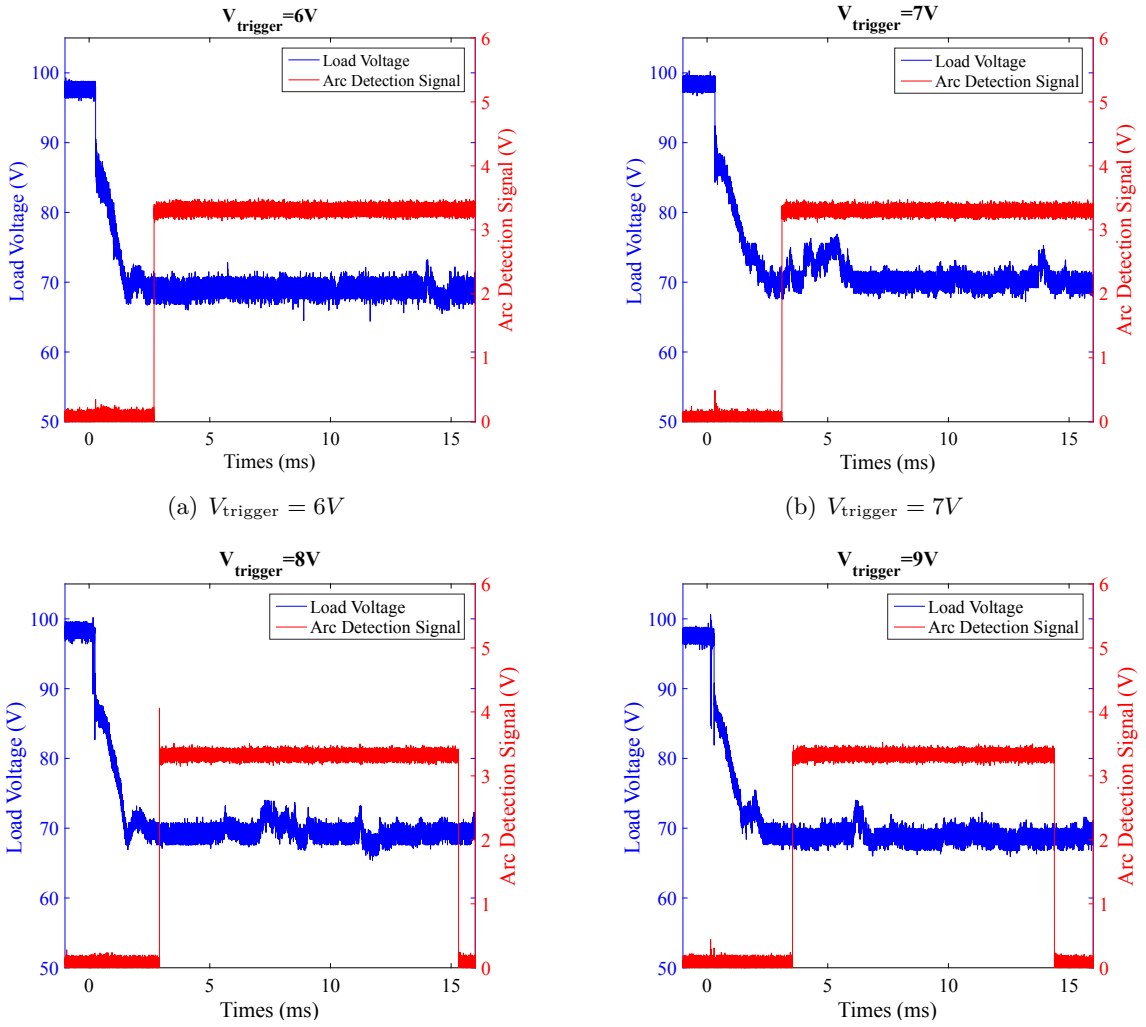

(a) $V_{\text{trigger}} = 6V$ (b) $V_{\text{trigger}} = 7V$

(c) $V_{\text{trigger}} = 8V$ (d) $V_{\text{trigger}} = 9V$

Figure 6-4: The experiment results for different threshold voltage of arc detection algorithm when $V_{\text{dc}} = 100V$, $I_{\text{load}} = 5A$, $L_{\text{cable}} = 200\mu H$ and $C_{\text{load}} = 0\mu F$.

The figures shown in Fig.6-5 and Fig.6-6 highlight the detection time with error-bar and detection rate during experiments under different circuit parameters.

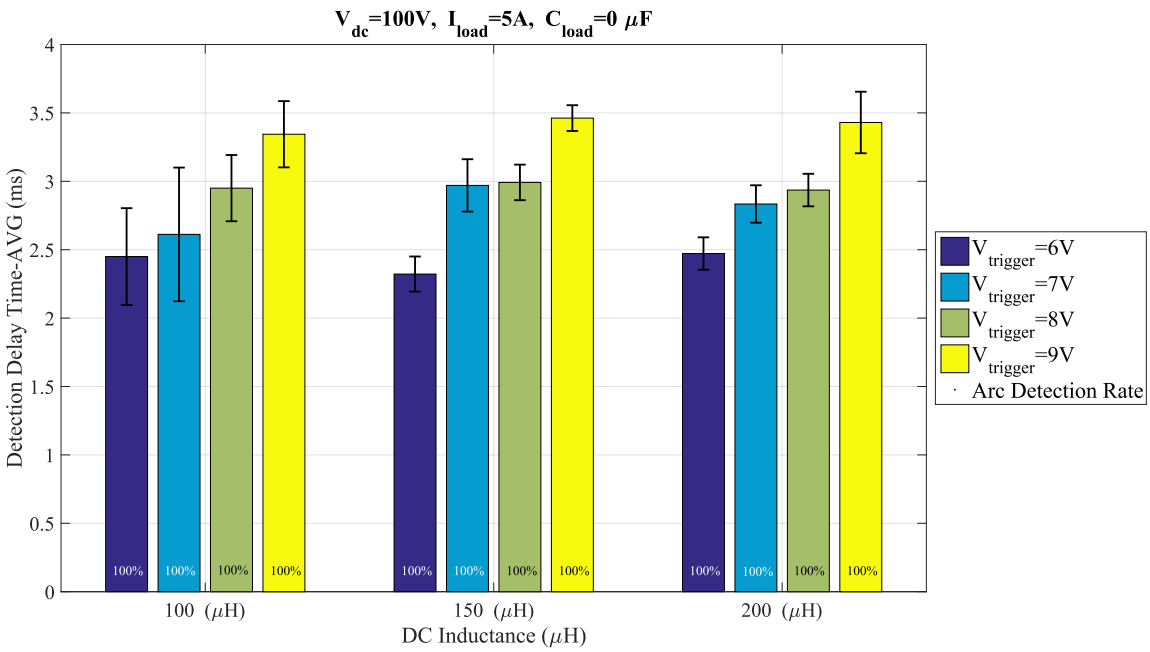

Figure 6-5: The arc detection response under different circuit parameters with $C_{\text{load}} = 0\mu F$.

As shown in Fig.6-5, the detection time for same trigger voltage under different inductance is almost same and experiences a rising trend with increasing the trigger voltage value (from around $2.46ms/6V$ to $3.39ms/9V$).

The same relationship between the detection time and trigger voltage can be observed in Fig.6-6. However what is more noteworthy is that with increasing load capacitance, the detection time under same trigger voltage decreases due to the load-side voltage amplification of capacitance which has been tested and explained in Chapter 5.

From all the experiment results, it can be summarized that: with increasing the value of trigger voltage (from $6V$ to $9V$), the detection time after arc initiation exposes the same rising tendency under different circuit parameter conditions, including the grid inductance and load capacitance.

According to the experiment results highlighted above, the series dc arc detection algorithm operates correctly and shows sensitivity, reliability and speed to detect the series dc arc fault in the circuit under different circuit conditions. The threshold voltage value has significant influence on the detection time, which should be taken into consideration of the determination of the trigger voltage to ensure the rapid detection and to avoid the spurious triggering.

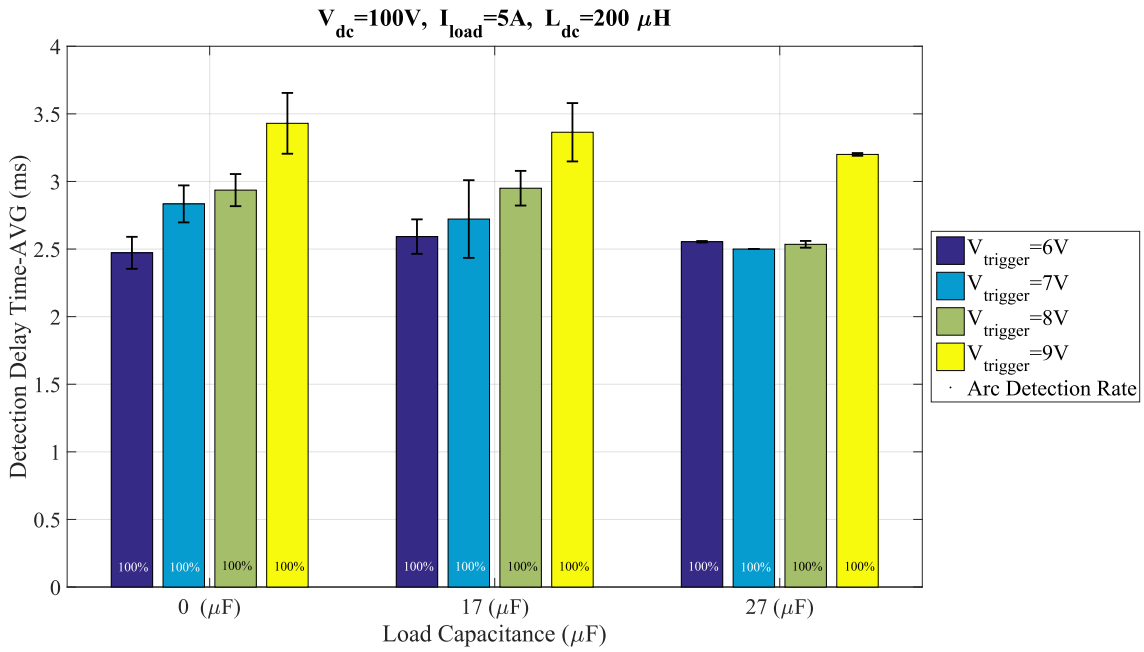

Figure 6-6: The arc detection response under different circuit parameters with $L_{\mathrm{dc}} = 200\mu H$.

6-4 Test on Selectivity

Moving further, as the sensitivity validation has been tested above, the selectivity of the arc detection algorithm will be examined and validated through the following experiments.

6-4-1 Setup and Procedure

According to the equivalent circuit shown in Fig.4-3, the experimental setup was built up as shown in Fig.6-7 with each load is equipped with arc detection algorithm for real-time arc detection, and the experiment parameters are listed in Table.6-3.

Table 6-3: Experiment Parameters for Selectivity Test.

Parameters	Symbol	Values
DC source voltage	V_{dc}	$100V$
Cable inductance	L_{dc}	$200\mu H$
Load capacitance	C_{load}	$0\mu F$, $17\mu F$, $27\mu F$
Arc current	I_{arc}	$5A$
Constant resistance load	R_{load}	Adjustable
Number of each test	n	10

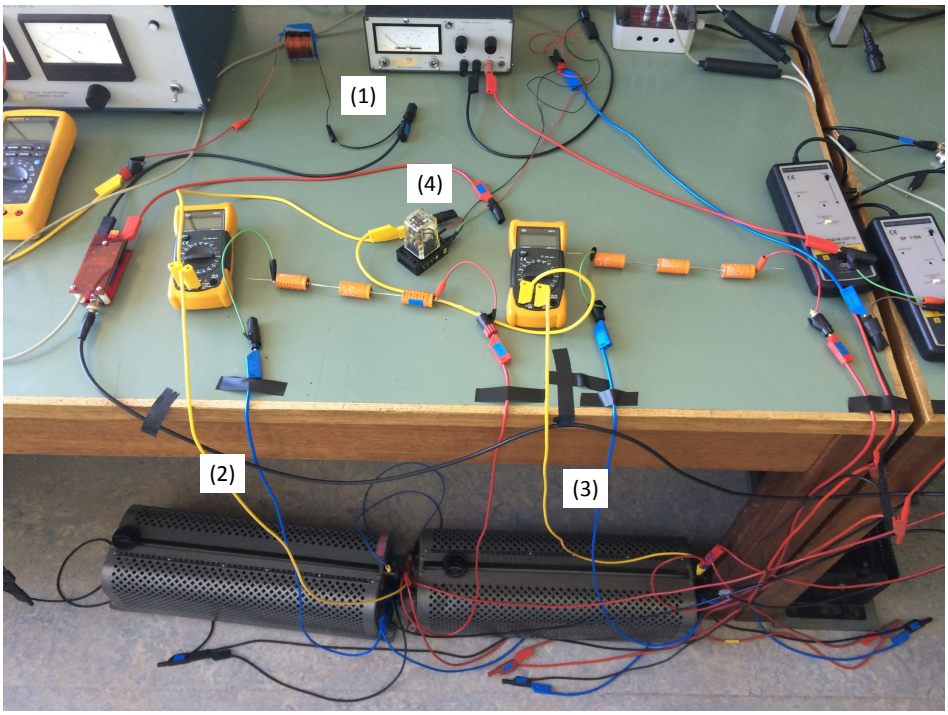

Figure 6-7: The practical setup with micro-controller for Selectivity Test, (1) Main line, (2) Branch 1, (3) Branch 2, (4) Arcing Relay.

Table 6-4: Detection Algorithm Parameters for Selectivity Tests [28].

Parameters	Symbol	Values
Slow LPF time constant	τ_{s}	$1ms$
Cascading Fast LPF time constant	τ_{f}	$0.1ms$
Trigger Voltage	V_{trigger}	$6V$

From the parameters table (Table.6-3), the dc voltage source supplies constant voltage at value of $100V$ to the loads through the $200\mu H$ inductance, and the capacitance which varies in three different values ($0\mu F$, $17\mu F$ and $27\mu F$) connects to the constant resistance load in parallel.

Additionally, the arc current (I_{arc}) means that load current of the line in which the arc fault will be imposes should be equals to $5A$ with aiming to raise the probability of arc generation and to make the arcing more sustainable and to last long enough till it can be detected.

Fig.6-8 shows the schematic diagram of the selectivity tests. As shown, there are three different position of arc, the selectivity of the detection algorithm can be validated by introducing the arc at different position of the system under different circuit parameters condition,

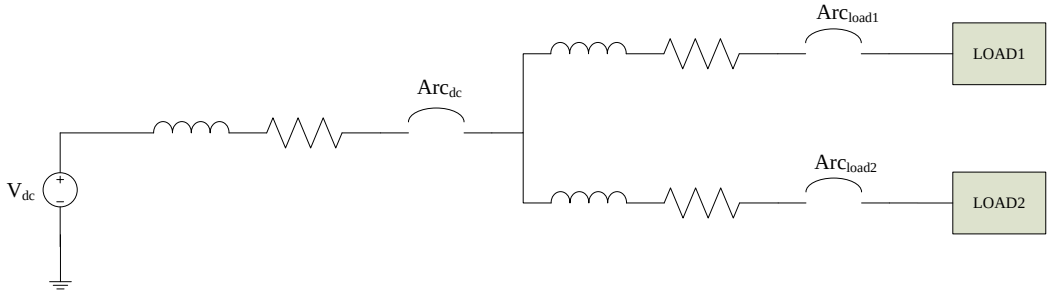

Figure 6-8: The schematic circuit diagram for selectivity tests.

and the expectation is that only the faulted line can trigger the arcing signal. Each condition was repeatedly tested for ten times.

By placing the arcing relay at the desired line in which the arcing fault is wanted, the realization of different arcing position can be achieved

During the experiments, the parameter of detection algorithm was kept as same as what was listed in Table.6-4, however only the $6V$ is chosen as the value of the trigger voltage for the arc detection algorithm.

For both load1 and load2, the load side voltage and the arc detection signal from the micro-controller are recorded by oscilloscope (YOKOGAWA DLM2054 mixed signal 2.5GS/s 500MHz) to check the experiment result directly.

6-4-2 Analysis of Experiment Results

A set of experiment has been performed with placing the arcing fault at different position in the circuit to examine the selectivity of the arc detection algorithm under different circuit parameters.

From Fig.6-9(a), it clearly shows that when the arcing fault occurs in branch line 1 (Arc_{load1}), only the load1-side arc detection signal is triggered in about $2.75ms$ after arc initiation, while no arc detection signal trigged for the load2.

While, similarly process presented in Fig.6-9(b), the trigger action happens only at load2-side arc detection signal when the arcing was introduced in branch2 (Arc_{load2}) with detection time for about $2.9ms$, while no reaction from load1-side detection.

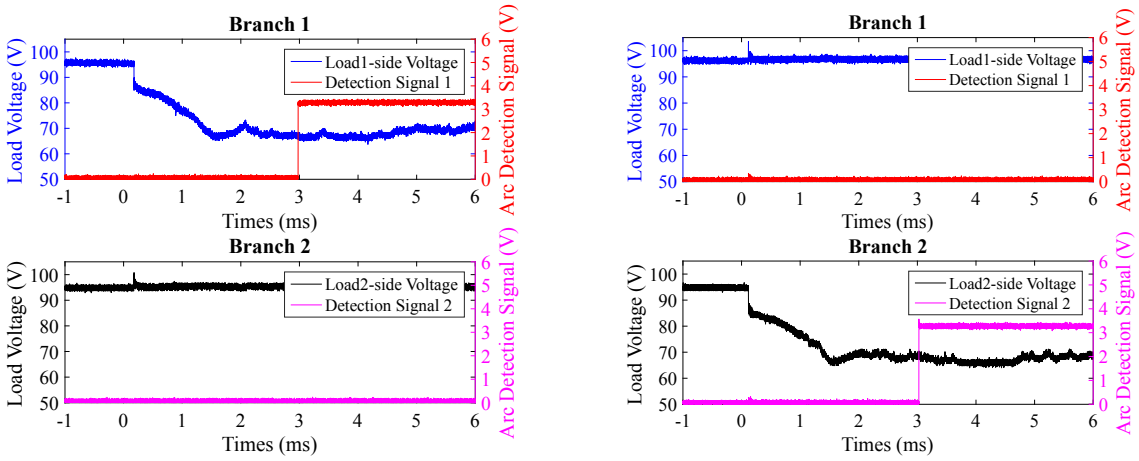

(a) Arcing at branch 1 (b) Arcing at branch 2

Figure 6-9: The response of detection algorithm to different arcing position.

Moving further, the arcing fault was introduced at DC main line (Arc_{dc}), and as expected, both the load1-side and load2-side arc detection signal were triggered almost at the same moment in around $2.65ms$ after arcing inception at dc side, which is presented in Fig.6-10.

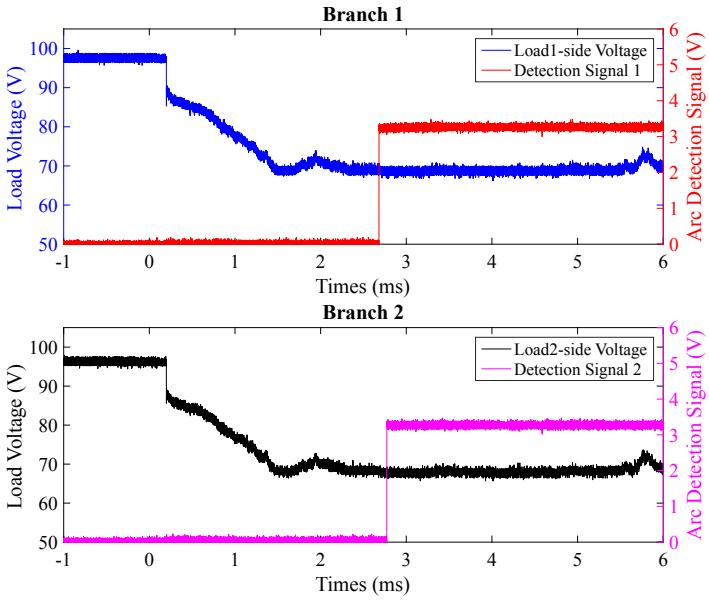

Figure 6-10: The response of detection algorithm to arcing at DC-side.

Next, the test for each arcing position under different circuit parameters has been repeated 10 times to check the reliability and selectivity of the detection algorithm. Besides no satisfied arcing initiated in case of $C_{\text{load}} = 27\mu F$, the experimental results were concluded in Table.6-5 and 6-6, and from them it can be seen that the arc detection algorithm reacts correctly for all the tests under different circuit parameters, which indicating that the selectivity of the series arc detection algorithm is achieved and guaranteed with reliability ensured.

Table 6-5: Arc Detection Rate for Selectivity Test with $C_{\text{load}} = 0\mu F$.

Arcing position	Load1-side Detection	Load2-side Detection
Branch line 1	100%	0%
Branch line 2	0%	100%
DC main line	100%	100%

Table 6-6: Arc Detection Rate for Selectivity Test with $C_{\text{load}} = 17\mu F$.

Arcing position	Load1-side Detection	Load2-side Detection
Branch line 1	100%	0%
Branch line 2	0%	100%
DC main line	100%	100%

6-5 Conclusion

The real time experimental validation for sensitivity and selectivity has been conducted by constructing the practical setup and programming the micro-controller and MATLAB for the achievement of the series dc arc detection algorithm in this chapter, and through the analysis of the experiment results gained from tests with changing both the trigger voltage value of the detection algorithm and the circuit parameters of the equivalent dc micro-grid system. The results has proved that the sensitivity, speed, reliability and selectivity has been harvested and safeguarded for the series dc arc detection algorithm in practical tests.

Chapter 7

Conclusion and Future Work

In this thesis, the arc detection algorithm has been explained and validated both in theoretical and practical way to guarantee the sensitivity, selectivity and speed.

First of all, the theoretical validation of the proposed series dc arc detection algorithm has been performed on the platform of Simulation in MATLAB by building the modeling of equivalent circuit and the arcing. And when there was series dc arc fault initiating at the DC-side in the dc micro-grids system especially under the condition of two constant power loads connected in parallel, the selectivity, localization and speed can be ensured.

Entering next stage, in order to investigate the impact of the external factors on the characteristic of the series dc arc, mainly on the load-side voltage drop and the corresponding time which are associated with the arc initiation, by varying the circuit parameters including the dc source voltage, the load current, the grid inductance and the input load capacitance, some experimental research on the series dc arc properties, like arc generation and sustainability have been designed and conducted, meanwhile the experimental results and the theory have been analysed and explained.

Finally, the real time experimental validation of the proposed series dc arc detection algorithm has also been performed via programming the micro-controller embedded with detection algorithm by changing the setting value of the trigger voltage, as a result, the applicability of the arc detection algorithm in the real arc fault detection in the power system network under different circuit parameters has been proved and verified with sensitivity, selectivity and speed given.

In order to make the series dc arc detection and elimination algorithm more completed and dependable, the further research can be performed on the validation of the series dc arc detection and elimination algorithm on these points:

- The circuit parameters, like the DC source voltage, load current, inductance and capacitance, can vary in wider range to enrich the experimental validation of the arc detection algorithm.
- The field test of the arc detection algorithm can be conducted in real dc micro-grid system.
- The insensitivity of the detection algorithm to the noise interference can be verified by performing the special real time experimental tests.
- The improvement on the band pass filter composed by slow LPF and fast LPF to ensure the robustness of the arc detection to the noise.
- The cooperation among different arc detection methods to facilitate the reliability of the arc detection.

In the foreseeable future, under the inevitable trend of increasing scale of renewable energy generation, energy storage and electrical vehicle, more and more dc micro-grids system will be designed and constructed around the whole world, and the arc detection technique will play an indispensable and important role in the application and operation of dc network.

Appendix A

Experiment Components Design

A-1 Inductor Design

Sometimes it is unable to find a inductor in particular value in the market. This is actually a problem faced by most of the electronic engineers, however the problem has become more and more serious if your project is RF related. The inductors required for RF circuits (antenna, tuner, amplifier etc.) are almost impossible to find in the present market and the only solution is nothing other than home-brewing the specific inductors.

The air-core inductor offer a solution to these problems with the advantages in cost-effectiveness and convenience without caring about the saturation occurs usually in the iron-core inductor.

With a little practice and patience you can construct air cored inductors with almost common value easily. The inductance of an air cored inductor can be represented using the simplified formula shown below in Equation.A-1 and to calculate the inductance of an air-core inductor, the same equation may be used.

$$L = \frac{\mu_0 A N^2}{l} \tag{A-1}$$

- L is the inductance (H);
- A is the surface area of the air coil (m^2);
- l is the length of the air coil (m);
- N is the number of turns.

There is something need to be noted: the length of the coil used in the inductor should be equal to or 0.4 times the diameter of the coil. And as shown in the equation, inductance of the

air-core inductor varies as the square of the number of turns. Thus the value l is multiplied four times if the value of n is doubled. The value of l is multiplied by two if the value of n is increased up to 40%.

The requirements listed in below for winding the coil should be obeyed carefully.

- The coil must be first wounded on a plastic former of the adequate diameter (equal to the required core diameter);
- The winding must be tight and adjacent turns must be as close as possible;
- After the winding is complete, slowly withdraw the core without disturbing the coil;
- Apply a thin layer of epoxy over the coil surface for mechanical support;
- Remove the insulation from the coil ends.

With the value of inductance, there comes with the parasitic resistance in the inductor on which some attention should be paid, and the smaller the value of parasitic resistance, the better the performance achieved by the air-core inductor designed and prepared.

Table A-1: Inductor Parameters Example.

Parameters	Values
Air Core diameter	$30mm$
Core length	$40mm$
Number of turns	67
Inductance	$100\mu H$

A-2 Voltage Divider Design

A voltage divider is a simple electrical circuit which turns a large voltage into a smaller one. Using just two series resistors and an input voltage, we can create an output voltage that is a fraction of the input. Voltage dividers are one of the most fundamental circuits in electronics.

The formula for calculating the output voltage is based on Ohms Law. The voltage division rule (voltage divider) is a simple rule which can be used in solving circuits to simplify the solution. The statement of the rule is simple: The voltage is divided between two series resistors in direct proportion to their resistance due to same current flows through the given resistors, voltage drop varies directly with its resistance in series circuit.

There are two important parts to the voltage divider: the circuit and the equation.

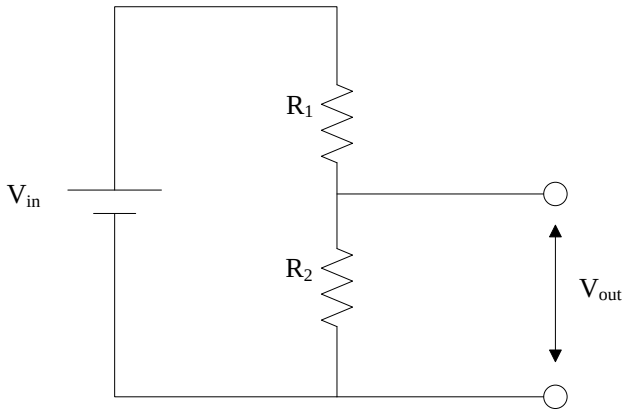

Figure A-1: The equivalent circuit diagram for voltage divider.

Fig.A-1 presents the diagram of a voltage divider that contains a high resistance across a voltage source, and the variable output voltage can be obtained across the resistance by varying value of R_2. This output voltage is a fraction of source voltage.

The resistor closest to the input voltage (V_{in}) is noted as R_1, and R_2 is for the resistor closest to ground. The voltage drop across R_2 is called V_{out}, that is the divided voltage our electrical circuit exists to make. V_{out} is the divided voltage being a fraction of the input voltage.

$$V_{\text{out}} = \frac{R_2}{R_1 + R_2} V_{\text{in}} \tag{A-2}$$

The voltage divider Equation shows that if the three values of the above circuit are known: the input voltage (V_{in}), and both resistor values (R_1 and R_2). Given those values, the output voltage (V_{out}) can be calculated by using this simple equation.

This equation states that the output voltage is directly proportional to the input voltage and the ratio of R_1 and R_2.

As for the particular voltage divider applied in this thesis, the transformer ratio of the voltage divider is $1000/3.3V$, which introducing the problem about the voltage constrain and the current constrain.

There should be a limitation on both voltage and the current suffered by each resistance

to restrict the breakthrough caused by the higher voltage or power losses in resistance. In this thesis, the method of ten potentiometer in each value of $10k\Omega$ connecting in series is applied to lower the voltage appears over each resistor and to limit the current goes through the voltage divider to reduce the heating power generated in each resistor.

Appendix B

Information of Micro-Controller

B-1 Introduction to Micro-controller and Code Composer Studio

The thesis chosen the LAUNCHXL-F28027F C2000 Piccolo LaunchPad experimenter kit designed and developed by Texas Instrument company as the micro-controller applied during the real-time experiments.

The C2000 Piccol LaunchPad, LAUNCHXL-F28027F, is a complete low-cost experimenter board for the Texas Instruments Piccolo F2802x devices. The LAUNCHXL-F28027F kit features all the hardware and software necessary to develop applications based on the F2802x microprocessor. The LaunchPad is based on the superset F28027F device, and easily allows users to migrate to lower cost F2802x devices once the design needs are known. It offers an on-board JTAG emulation tool allowing direct interface to a PC for easy programming, debugging, and evaluation. In addition to JTAG emulation, the USB interface provides a UART serial connection from the F2802x device to the host PC.

Meanwhile, the Code Composer Studio IDE version 6 can be download from the C2000 LaunchPad page (http://www.ti.com/c2000-launchpad) by users without any constrains to write, download, and debug applications on the LAUNCHXL-F28027F board. The debugger is unobtrusive, allowing the user to run an application at full speed with hardware breakpoints and single stepping available while consuming no extra hardware resources.

The Code Composer Studio is an integrated development environment (IDE) that supports TI's microcontroller and embedded processors portfolio. Code Composer Studio comprises a suite of tools used to develop and debug embedded applications. It includes an optimizing C/C++ compiler, source code editor, project build environment, debugger, profiler, and many other features. The intuitive IDE provides a single user interface taking you through

each step of the application development flow. Familiar tools and interfaces allow users to get started faster than ever before. Code Composer Studio combines the advantages of the Eclipse software framework with advanced embedded debug capabilities from TI resulting in a compelling feature-rich development environment for embedded developers. The Code Composer Studio IDE is available for free without any restriction when used with the XDS100 emulator on the C2000 LaunchPad. At this site, you can also download a copy of controlSUITE that includes drivers, examples, and other support software needed to get started.

The C2000 LaunchPad installation consists of three easy steps:

1. Download Code Composer Studio and controlSUITE;
2. Install Code Composer Studio and controlSUITE;
3. Connect and install the C2000 LaunchPad to the PC.

After the steps above accomplished, the LaunchPad is ready to develop applications or run the programmed burned-in by plugging the supplied USB cable into the C2000 LaunchPad board and into an available USB port on your computer. Windows will automatically detect the hardware and ask you to install software drivers. Let Windows run a search for the drivers and automatically install them. After Windows successfully installs the drivers for the integrated XDS100v2 emulator, your LaunchPad is now ready for use. The first time the LAUNCHXL-F28027F is used, a demo application automatically starts when the board is powered from a USB host. If your board does not start the demo application, try placing S1 in the following positions and resetting the board: UP-UP-DOWN. To start the demo, connect the LAUNCHXL-F28027F with the included mini-USB cable to a free USB port. The demo application starts with the LEDs flashing to show the device is active. The C2000 LaunchPad gives users several options as to how to configure the board.

1. Power Domain

   The C2000 LaunchPad has two separate power domains for the purpose of allowing JTAG isolation. Jumpers JP1, JP2, and JP3 configure whether the USB power is passed to the target device.

2. Serial Connectivity

   The LAUNCHXL-F28027F has a USB to UART adapter built in. This makes it easy to print debug information back to the host PC even in isolated environments. However, in some cases the user may wish to connect the Piccolo SCI peripheral (C2000 UART peripheral) to a Booster-Pack or other hardware via the header pins. If the SCI pins are connected to both the header pins, the XDS100 UART channel contention would exist and the pins would not be driven to the correct voltage levels. To solve this issue we have included a switch to allow the user to disconnect the Piccolo serial pins from the XDS100 UART connection. When S4 is in the up position, the Piccolo device's

SCI is connected to the XDS100 and you are able to receive and send serial information from or to the board. When S4 is in the down position, the Piccolo device's SCI is disconnected from the XDS100 and Booster-Packs, which use serial communication, and can communicate with the Piccolo device.

3. Boot Mode Selection

   The LaunchPad's F28027F device includes a boot ROM that performs some basic start-up checks and allows for the device to boot in many different ways. Most users will either want to perform an emulation boot or a boot to flash (if they are running the application standalone). S1 has been provided to allow users to easily configure the pins that the boot ROM checks to make this decision.

4. Connecting a Crystal

   Although the Piccolo device present on the LAUNCHXL-F28027F has an internal oscillator and for most applications this is sufficient, the LaunchPad offers a footprint for surface mount or through-hole HC-49 crystals for users who require a more precise clock. If you wish to use an external crystal, solder the crystal to the Q1/Q2 footprint and appropriate load capacitors to the C3 and C4 footprints. You also need to configure the device to use the external oscillator in software.

5. Connecting a Satellite Board

   The C2000 LaunchPad is the perfect experimenter board to start hardware development with the F2802x devices. Connectors J1, J2, J5, and J6 and the power supply at J3 are aligned in a 0.1-in (2.54-mm) grid to allow an easy and inexpensive development of a breadboard extension module. These satellite boards can access all of the GPIO and analog signals.

6. Device Migration Path

   Applications developed on the LAUNCHXL-F28027F can easily be migrated to any of these lower cost devices in the F2802x family.

B-2 Configuration between Micro-controller and MATLAB Simulink

Embedded Coder Support Package for Texas Instruments C2000 Processors enables you to generate a real-time executable, and download it to your TI development board. Embedded Coder automatically generates C code and inserts the I/O device drivers in your block diagram. These device drivers are inserted in the generated C code.

MATLAB Coder, Simulink Coder, and Embedded Coder generate ANSI/ISO C/C++ code that can be compiled and executed on Texas Instruments Piccolo F28x 32-bit microcontrollers. Embedded Coder lets you easily configure the code generated from MATLAB and Simulink

algorithms to control software interfaces, optimize execution performance, and minimize memory consumption. Embedded Coder provides additional support for the Piccolo F28x 32-bit microcontrollers that includes automated build and execution, processor-optimized code, ability to perform processor-in-the-loop (PIL) tests with execution profiling, block libraries for on-chip and on-board peripherals, and deployment support using built-in scheduler.

Before you install the software, if you install the Texas Instruments (TI) Code Composer Studio CCSv3 on Windows, then, make sure that:

- You have administrator privileges;
- You have set the User Account Control (UAC) settings to the lowest level;
- You install CCSv.6.0.0 in a folder other than Program Files.

Using this installation process, you download and install the following items on your host computer:

- Support for Texas Instruments C2000 processors and its features;
- Simulink block library Embedded Coder Support Package for Texas Instruments C2000 Processors;
- Examples that show you how to use the Texas Instruments C2000 processor.

With entering into next stage at which hardware implementation is parameterized for creating and sunning applications on target hardware, the configuration should be done in Simulink by the following steps:

1. In the Simulink Editor, select Simulink>Model Configuration Parameter;
2. In the Configuration Parameter dialog box, click Hardware Implementation;
3. Set the Hardware board parameter to match your C2000 processor;
4. Click Apply to apply the changes.

In the Hardware board pane, it is important to select the type of hardware on which to run your model, because changing this parameter updates the Configuration Parameters dialog and it only displays parameters that are relevant to your target hardware.

After installing support for your target hardware, reopen the Configuration Parameters dialog and select your target hardware. And then, selecting the appropriate C2000 processor option to run the model on your micro-controller with C2000 processor.

Appendix C

Coding for Matlab and Micro-Controller

C-1 Coding in MATLAB

C-1-1 Arc Resistance Coding

```
if L>0;
    V_arc=13.3;
    X=[0 1 5 10 20 50 100 200];
    Y=[V_arc/I_arc 36.32*I_arc^(-1.124) 71.39*I_arc^(-1.186) 105.25*I_arc
       ^(-1.239) 153.63*I_arc^(-1.278) 262.02*I_arc^(-1.310) 481.20*I_arc
       ^(-1.350) 662.34*I_arc^(-1.283)];
    R_arc=interp1(X,Y,L,'linear');
else
    R_arc=0;
end
```

C-1-2 Current Elimination Algorithm Coding

```
if S==10;
    if I_load>0;
        I_load1=I_load-700*t;
        if I_load1>0;
            I_load2=I_load1;
%             test=I_load2
        else
            I_load2=0;
        end
```

```
    else
        I_load2=0;
    end
else
    I_load2=I_load;
end
```

C-2 TMS320f28027f Detection Algorithm Coding in C language

```
/*
 * Academic License - for use in teaching, academic research, and meeting
 * course requirements at degree granting institutions only.  Not for
 * government, commercial, or other organizational use.
 *
 * File: test_adc2sci_0617HB_Double_0705.c
 *
 * Code generated for Simulink model 'test_adc2sci_0617HB_Double_0705'.
 *
 * Model version                  : 1.241
 * Simulink Coder version         : 8.9 (R2015b) 13-Aug-2015
 * C/C++ source code generated on : Fri Jul 15 12:34:13 2016
 *
 * Target selection: ert.tlc
 * Embedded hardware selection: Texas Instruments->C2000
 * Code generation objectives: Unspecified
 * Validation result: Not run
 */

#include "test_adc2sci_0617HB_Double_0705.h"
#include "test_adc2sci_0617HB_Double_0705_private.h"

/* Block signals (auto storage) */
B_test_adc2sci_0617HB_Double__T test_adc2sci_0617HB_Double_07_B;

/* Block states (auto storage) */
DW_test_adc2sci_0617HB_Double_T test_adc2sci_0617HB_Double_0_DW;

/* Real-time model */
RT_MODEL_test_adc2sci_0617HB__T test_adc2sci_0617HB_Double_0_M_;
RT_MODEL_test_adc2sci_0617HB__T *const test_adc2sci_0617HB_Double_0_M =
  &test_adc2sci_0617HB_Double_0_M_;

/*
 * Output and update for atomic system:
 *    '<Root>/MATLAB Function'
 *    '<Root>/MATLAB Function1'
 */
```

```
39 void test_adc2sci_061_MATLABFunction(real_T rtu_vload, real_T rtu_DT,
       real_T
40   rtu_V_trigger, real_T rtu_V_slpf_pre, real_T rtu_V_flpf1_pre, real_T
41   rtu_V_flpf2_pre, B_MATLABFunction_test_adc2sci_T *localB)
42 {
43   real_T Alpha_slpf;
44   real_T Alpha_flpf;
45   real_T V_flpf1;
46
47   /* MATLAB Function 'MATLAB Function': '<S1>:1' */
48   /* % Input the setting value for the Detection Algorithm */
49   /*  setting value for the sample time */
50   /*  DT=4e-5;  %  (s) */
51   /*  DT=0.001; */
52   /*  setting value for the time constant for different LPF */
53   /*  group1 */
54   /*  Tau_slpf=0.4;    % time constant for Slow LPF (s) */
55   /*  Tau_flpf=0.001;  % time constant for Fast LPF (s) */
56   /*  group 2 */
57   /* '<S1>:1:16' */
58   /*  time constant for Slow LPF (s) */
59   /* '<S1>:1:17' */
60   /*  time constant for Fast LPF (s) */
61   /*  calculating for smoothing factor */
62   /* '<S1>:1:20' */
63   Alpha_slpf = rtu_DT / (rtu_DT + 0.001);
64
65   /*  smoothing factor for Slow LPF */
66   /* '<S1>:1:21' */
67   Alpha_flpf = rtu_DT / (rtu_DT + 0.0001);
68
69   /*  smoothing factor for Fast LPF */
70   /*  setting value for the initial signal */
71   /* '<S1>:1:25' */
72   localB->signal = 0.0;
73
74   /* % Detection Algorithm Function */
75   /* '<S1>:1:28' */
76   Alpha_slpf = (1.0 - Alpha_slpf) * rtu_V_slpf_pre + Alpha_slpf *
       rtu_vload;
77
78   /*  output from Slow LPF  */
79   /* '<S1>:1:29' */
80   V_flpf1 = (1.0 - Alpha_flpf) * rtu_V_flpf1_pre + Alpha_flpf * rtu_vload
       ;
81
82   /*  output from Fast LPF */
83   /* '<S1>:1:30' */
```

```
84    Alpha_flpf = (1.0 - Alpha_flpf) * rtu_V_flpf2_pre + Alpha_flpf *
          V_flpf1;
85
86    /*  output from 2 cascading Fast LPF  */
87    /* '<S1>:1:32' */
88    localB->V_slpf_aft = Alpha_slpf;
89
90    /* '<S1>:1:33' */
91    localB->V_flpf1_aft = V_flpf1;
92
93    /* '<S1>:1:34' */
94    localB->V_flpf2_aft = Alpha_flpf;
95
96    /* '<S1>:1:36' */
97    /*  pay attention on Fast LPF is cascading or not to change the
          subscript number of the V_flpf(x) */
98    if (Alpha_slpf - Alpha_flpf >= rtu_V_trigger) {
99      /* '<S1>:1:39' */
100     /*  decide the detection signal */
101     /* '<S1>:1:40' */
102     localB->signal = 1.0;
103
104     /*  set value to signal when arc is detected */
105   }
106 }
107
108 real_T rt_roundd_snf(real_T u)
109 {
110   real_T y;
111   if (fabs(u) < 4.503599627370496E+15) {
112     if (u >= 0.5) {
113       y = floor(u + 0.5);
114     } else if (u > -0.5) {
115       y = u * 0.0;
116     } else {
117       y = ceil(u - 0.5);
118     }
119   } else {
120     y = u;
121   }
122
123   return y;
124 }
125
126 /* Model step function */
127 void test_adc2sci_0617HB_Double_0705_step(void)
128 {
129   real_T tmp;
```

```
130
131   /* S-Function (c2802xadc): '<Root>/ADC' */
132   {
133     /*  Internal Reference Voltage : Fixed scale 0 to 3.3 V range.  */
134     /*  External Reference Voltage : Allowable ranges of VREFHI(ADCINA0)
          = 3.3 and VREFLO(tied to ground) = 0  */
135     AdcRegs.ADCSOCFRC1.bit.SOC0 = 1;
136     asm(" RPT #22 || NOP");
137     test_adc2sci_0617HB_Double_07_B.ADC = (AdcResult.ADCRESULT0);
138   }
139
140   /* MATLAB Function: '<Root>/MATLAB Function' incorporates:
141    *  Constant: '<Root>/Sample Time'
142    *  Constant: '<Root>/Trigger Voltage'
143    *  UnitDelay: '<Root>/Fast LPF1'
144    *  UnitDelay: '<Root>/Fast LPF2'
145    *  UnitDelay: '<Root>/Slow LPF'
146    */
147   test_adc2sci_061_MATLABFunction(test_adc2sci_0617HB_Double_07_B.ADC,
148     test_adc2sci_0617HB_Double_07_P.sampletime,
149     test_adc2sci_0617HB_Double_07_P.V_trigger,
150     test_adc2sci_0617HB_Double_0_DW.SlowLPF_DSTATE,
151     test_adc2sci_0617HB_Double_0_DW.FastLPF1_DSTATE,
152     test_adc2sci_0617HB_Double_0_DW.FastLPF2_DSTATE,
153     &test_adc2sci_0617HB_Double_07_B.sf_MATLABFunction);
154
155   /* S-Function (c280xgpio_do): '<Root>/Digital Output' */
156   {
157     GpioDataRegs.GPASET.bit.GPIO3 =
158       (test_adc2sci_0617HB_Double_07_B.sf_MATLABFunction.signal != 0);
159     GpioDataRegs.GPACLEAR.bit.GPIO3 =
160       !(test_adc2sci_0617HB_Double_07_B.sf_MATLABFunction.signal != 0);
161   }
162
163   /* DataTypeConversion: '<Root>/Data Type Conversion' */
164   tmp = rt_roundd_snf(test_adc2sci_0617HB_Double_07_B.ADC);
165   if (rtIsNaN(tmp) || rtIsInf(tmp)) {
166     tmp = 0.0;
167   } else {
168     tmp = fmod(tmp, 4.294967296E+9);
169   }
170
171   test_adc2sci_0617HB_Double_07_B.DataTypeConversion = tmp < 0.0 ? -(
        int32_T)
172     (uint32_T)-tmp : (int32_T)(uint32_T)tmp;
173
174   /* End of DataTypeConversion: '<Root>/Data Type Conversion' */
175
```

```
176   /* S-Function (c28xsci_tx): '<Root>/SCI Transmit' */
177   {
178     /* Send additional data header */
179     {
180       char *String = "S";
181       scia_xmit(String, 1, 1);
182     }
183
184     scia_xmit((char*)&test_adc2sci_0617HB_Double_07_B.DataTypeConversion,
          4, 4);
185
186     /* Send additional data terminator */
187     {
188       char *String = "E";
189       scia_xmit(String, 1, 1);
190     }
191   }
192
193   /* S-Function (c2802xadc): '<Root>/ADC1' */
194   {
195     /*  Internal Reference Voltage : Fixed scale 0 to 3.3 V range.  */
196     /*  External Reference Voltage : Allowable ranges of VREFHI(ADCINA0)
          = 3.3 and VREFLO(tied to ground) = 0  */
197     AdcRegs.ADCSOCFRC1.bit.SOC1 = 1;
198     asm(" RPT #22 || NOP");
199     test_adc2sci_0617HB_Double_07_B.ADC1 = (AdcResult.ADCRESULT1);
200   }
201
202   /* MATLAB Function: '<Root>/MATLAB Function1' incorporates:
203    *  Constant: '<Root>/Sample Time1'
204    *  Constant: '<Root>/Trigger Voltage1'
205    *  UnitDelay: '<Root>/Fast LPF3'
206    *  UnitDelay: '<Root>/Fast LPF4'
207    *  UnitDelay: '<Root>/Slow LPF1'
208    */
209   test_adc2sci_061_MATLABFunction(test_adc2sci_0617HB_Double_07_B.ADC1,
210     test_adc2sci_0617HB_Double_07_P.sampletime,
211     test_adc2sci_0617HB_Double_07_P.V_trigger,
212     test_adc2sci_0617HB_Double_0_DW.SlowLPF1_DSTATE,
213     test_adc2sci_0617HB_Double_0_DW.FastLPF3_DSTATE,
214     test_adc2sci_0617HB_Double_0_DW.FastLPF4_DSTATE,
215    &test_adc2sci_0617HB_Double_07_B.sf_MATLABFunction1);
216
217   /* S-Function (c280xgpio_do): '<Root>/Digital Output1' */
218   {
219     GpioDataRegs.GPASET.bit.GPIO2 =
220       (test_adc2sci_0617HB_Double_07_B.sf_MATLABFunction1.signal != 0);
221     GpioDataRegs.GPACLEAR.bit.GPIO2 =
```

```
222         !(test_adc2sci_0617HB_Double_07_B.sf_MATLABFunction1.signal != 0);
223     }
224
225     /* Update for UnitDelay: '<Root>/Slow LPF' */
226     test_adc2sci_0617HB_Double_0_DW.SlowLPF_DSTATE =
227       test_adc2sci_0617HB_Double_07_B.sf_MATLABFunction.V_slpf_aft;
228
229     /* Update for UnitDelay: '<Root>/Fast LPF1' */
230     test_adc2sci_0617HB_Double_0_DW.FastLPF1_DSTATE =
231       test_adc2sci_0617HB_Double_07_B.sf_MATLABFunction.V_flpf1_aft;
232
233     /* Update for UnitDelay: '<Root>/Fast LPF2' */
234     test_adc2sci_0617HB_Double_0_DW.FastLPF2_DSTATE =
235       test_adc2sci_0617HB_Double_07_B.sf_MATLABFunction.V_flpf2_aft;
236
237     /* Update for UnitDelay: '<Root>/Slow LPF1' */
238     test_adc2sci_0617HB_Double_0_DW.SlowLPF1_DSTATE =
239       test_adc2sci_0617HB_Double_07_B.sf_MATLABFunction1.V_slpf_aft;
240
241     /* Update for UnitDelay: '<Root>/Fast LPF3' */
242     test_adc2sci_0617HB_Double_0_DW.FastLPF3_DSTATE =
243       test_adc2sci_0617HB_Double_07_B.sf_MATLABFunction1.V_flpf1_aft;
244
245     /* Update for UnitDelay: '<Root>/Fast LPF4' */
246     test_adc2sci_0617HB_Double_0_DW.FastLPF4_DSTATE =
247       test_adc2sci_0617HB_Double_07_B.sf_MATLABFunction1.V_flpf2_aft;
248 }
249
250 /* Model initialize function */
251 void test_adc2sci_0617HB_Double_0705_initialize(void)
252 {
253     /* Registration code */
254
255     /* initialize non-finites */
256     rt_InitInfAndNaN(sizeof(real_T));
257
258     /* initialize error status */
259     rtmSetErrorStatus(test_adc2sci_0617HB_Double_0_M, (NULL));
260
261     /* block I/O */
262     (void) memset(((void *) &test_adc2sci_0617HB_Double_07_B), 0,
263                   sizeof(B_test_adc2sci_0617HB_Double__T));
264
265     /* states (dwork) */
266     (void) memset((void *)&test_adc2sci_0617HB_Double_0_DW, 0,
267                   sizeof(DW_test_adc2sci_0617HB_Double_T));
268
269     /* Start for S-Function (c2802xadc): '<Root>/ADC' */
```

```
270   InitAdc();
271   config_ADC_SOC0 ();
272
273   /* Start for S-Function (c280xgpio_do): '<Root>/Digital Output' */
274   EALLOW;
275   GpioCtrlRegs.GPAMUX1.all &= 0xFFFFFF3F;
276   GpioCtrlRegs.GPADIR.all |= 0x8;
277   EDIS;
278
279   /* Start for S-Function (c2802xadc): '<Root>/ADC1' */
280   config_ADC_SOC1 ();
281
282   /* Start for S-Function (c280xgpio_do): '<Root>/Digital Output1' */
283   EALLOW;
284   GpioCtrlRegs.GPAMUX1.all &= 0xFFFFFFCF;
285   GpioCtrlRegs.GPADIR.all |= 0x4;
286   EDIS;
287
288   /* InitializeConditions for UnitDelay: '<Root>/Slow LPF' */
289   test_adc2sci_0617HB_Double_0_DW.SlowLPF_DSTATE =
290     test_adc2sci_0617HB_Double_07_P.V_slpf_initial;
291
292   /* InitializeConditions for UnitDelay: '<Root>/Fast LPF1' */
293   test_adc2sci_0617HB_Double_0_DW.FastLPF1_DSTATE =
294     test_adc2sci_0617HB_Double_07_P.V_flpf_initial;
295
296   /* InitializeConditions for UnitDelay: '<Root>/Fast LPF2' */
297   test_adc2sci_0617HB_Double_0_DW.FastLPF2_DSTATE =
298     test_adc2sci_0617HB_Double_07_P.V_flpf_initial;
299
300   /* InitializeConditions for UnitDelay: '<Root>/Slow LPF1' */
301   test_adc2sci_0617HB_Double_0_DW.SlowLPF1_DSTATE =
302     test_adc2sci_0617HB_Double_07_P.V_slpf_initial;
303
304   /* InitializeConditions for UnitDelay: '<Root>/Fast LPF3' */
305   test_adc2sci_0617HB_Double_0_DW.FastLPF3_DSTATE =
306     test_adc2sci_0617HB_Double_07_P.V_flpf_initial;
307
308   /* InitializeConditions for UnitDelay: '<Root>/Fast LPF4' */
309   test_adc2sci_0617HB_Double_0_DW.FastLPF4_DSTATE =
310     test_adc2sci_0617HB_Double_07_P.V_flpf_initial;
311 }
312
313 /* Model terminate function */
314 void test_adc2sci_0617HB_Double_0705_terminate(void)
315 {
316   /* (no terminate code required) */
317 }
```

```
318
319 /*
320  * File trailer for generated code.
321  *
322  * [EOF]
323  */
```

Bibliography

[1] K. J. Lee, G. S. Seo, and B. H. Cho, "Dc arc fault detection method for dc microgrid using branch monitoring," in *2015 9th International Conference on Power Electronics and ECCE Asia (ICPE-ECCE Asia)*, pp. 2079–2084, June 2015.

[2] J. D. Park and J. Candelaria, "Fault detection and isolation in low-voltage dc-bus microgrid system," *IEEE Transactions on Power Delivery*, vol. 28, pp. 779–787, April 2013.

[3] X. Yao, L. Herrera, and J. Wang, "Impact evaluation of series dc arc faults in dc microgrids," in *2015 IEEE Applied Power Electronics Conference and Exposition (APEC)*, pp. 2953–2958, March 2015.

[4] H. C. Su, G. W. Chang, B. W. Liu, J. H. Chen, K. K. Jen, C. H. Chung, and J. Z. Wu, "Modeling and simulation for grid fault impacts on a dc microgrid," in *Computer, Consumer and Control (IS3C), 2012 International Symposium on*, pp. 373–376, June 2012.

[5] K. J. Tseng and G. Luo, "Power electronic-based protection for direct-current power distribution in micro-grids," in *2014 International Power Electronics Conference (IPEC-Hiroshima 2014 - ECCE ASIA)*, pp. 2145–2151, May 2014.

[6] C. Yuan, M. A. Haj-ahmed, and M. S. Illindala, "Protection strategies for medium-voltage direct-current microgrid at a remote area mine site," *IEEE Transactions on Industry Applications*, vol. 51, pp. 2846–2853, July 2015.

[7] D. M. Bui, S. L. Chen, C. H. Wu, K. Y. Lien, C. H. Huang, and K. K. Jen, "Review on protection coordination strategies and development of an effective protection coordination system for dc microgrid," in *2014 IEEE PES Asia-Pacific Power and Energy Engineering Conference (APPEEC)*, pp. 1–10, Dec 2014.

[8] G. Patil and M. F. A. R. Satarkar, "Autonomous protection of low voltage dc microgrid," in *Power, Automation and Communication (INPAC), 2014 International Conference on*, pp. 23–26, Oct 2014.

[9] D. Salomonsson, L. Soder, and A. Sannino, "Protection of low-voltage dc microgrids," *IEEE Transactions on Power Delivery*, vol. 24, pp. 1045–1053, July 2009.

[10] G. S. Seo, K. A. Kim, K. C. Lee, K. J. Lee, and B. H. Cho, "A new dc arc fault detection method using dc system component modeling and analysis in low frequency range," in *2015 IEEE Applied Power Electronics Conference and Exposition (APEC)*, pp. 2438–2444, March 2015.

[11] X. Yao, L. Herrera, S. Ji, K. Zou, and J. Wang, "Characteristic study and time-domain discrete- wavelet-transform based hybrid detection of series dc arc faults," *IEEE Transactions on Power Electronics*, vol. 29, pp. 3103–3115, June 2014.

[12] G. S. Seo, J. I. Ha, B. H. Cho, and K. C. Lee, "Series arc fault detection method based on statistical analysis for dc microgrids," in *2016 IEEE Applied Power Electronics Conference and Exposition (APEC)*, pp. 487–492, March 2016.

[13] S. Guo, J. Jones, and A. Dooley, "Dc arc detection and prevention circuit and method," Jan. 27 2004. US Patent 6,683,766.

[14] M. Dargatz and M. Fornage, "Method and apparatus for detection and control of dc arc faults," May 15 2012. US Patent 8,179,147.

[15] J. Zuercher, J. Hastings, E. Hetzmannseder, J. Pardee, and C. Tennies, "Detection of arcing in dc electrical systems," Feb. 12 2004. US Patent App. 10/416,611.

[16] L. Mackay, A. Shekhar, B. Roodenburg, L. Ramirez-Elizondo, and P. Bauer, "Series arc extinction in dc microgrids using load side voltage drop detection," in *DC Microgrids (ICDCM), 2015 IEEE First International Conference on*, pp. 239–244, June 2015.

[17] A. Shekhar, *Detection, characterization and extinction of electric arcs in DC Systems*. PhD thesis, TU Delft, Delft University of Technology, 2015.

[18] L. Van der Sluis, *Transients in power systems*, vol. 2001. Wiley New York, 2001.

[19] L. Yuan, J. Shengchang, W. Jin, Y. Xiu, and Z. Yeye, "Study on characteristics and detection of dc arc fault in power electronics system," in *Condition Monitoring and Diagnosis (CMD), 2012 International Conference on*, pp. 1043–1046, Sept 2012.

[20] F. M. Uriarte, A. L. Gattozzi, J. D. Herbst, H. B. Estes, T. J. Hotz, A. Kwasinski, and R. E. Hebner, "A dc arc model for series faults in low voltage microgrids," *IEEE Transactions on Smart Grid*, vol. 3, pp. 2063–2070, Dec 2012.

[21] J. Li, D. W. P. Thomas, M. Sumner, E. Christopher, and Y. Cao, "Series arc fault studies and modeling for a dc distribution system," in *2013 IEEE PES Asia-Pacific Power and Energy Engineering Conference (APPEEC)*, pp. 1–6, Dec 2013.

[22] R. F. Ammerman, T. Gammon, P. K. Sen, and J. P. Nelson, "Dc-arc models and incident-energy calculations," *IEEE Transactions on Industry Applications*, vol. 46, pp. 1810–1819, Sept 2010.

[23] X. Yao, L. Herrera, Y. Huang, and J. Wang, "The detection of dc arc fault: Experimental study and fault recognition," in *2012 Twenty-Seventh Annual IEEE Applied Power Electronics Conference and Exposition (APEC)*, pp. 1720–1727, Feb 2012.

[24] X. Yao, L. Herrera, and J. Wang, "A series dc arc fault detection method and hardware implementation," in *Applied Power Electronics Conference and Exposition (APEC), 2013 Twenty-Eighth Annual IEEE*, pp. 2444–2449, March 2013.

[25] Y. Cao, J. Li, M. Sumner, E. Christopher, and D. Thomas, "Arc fault generation and detection in dc systems," in *2013 IEEE PES Asia-Pacific Power and Energy Engineering Conference (APPEEC)*, pp. 1–5, Dec 2013.

[26] A. Shekhar, L. Mackay, L. Ramirez-Elizondo, and P. Bauer, "Experimental design of a series arc load side detection algorithm for dc microgrid protection," in *2016 International Symposium on Power Electronics, Electrical Drives, Automation and Motion (SPEEDAM)*, pp. 343–347, June 2016.

[27] J. Paukert, "The arc voltage and the resistance of lv fault arcs," in *7th International Symposium on Switching Arc Phenomena, TU Lodz, Poland*, pp. 49–51, 1993.

[28] A. Shekhar, L. Mackay, L. Ramirez-Elizondo, and P. Bauer, "Dc microgrid protection by selective detection of series arcing using load side power electronic devices," in *Power Electronics and Applications (EPE), 18th European Conference on, Karlsruhe, Germany*, June 2016.

Glossary

List of Acronyms

ac	Alternating Current
dc	Direct Current
LPF	Low Pass Filter
LV	Low Voltage
RLC	Resistance, Inductance and Capacitance